

FABRICATION AND MAGNETIC PROPERTIES
OF PATTERNED THIN FILMS

THESIS

Presented to the Graduate Council of
Southwest Texas State University

In Partial Fulfillment of
the Requirements

For the Degree
Master of Science

By
Claude H. Garrett IV

San Marcos, Texas

May, 2002

ACKNOWLEDGEMENTS

I would like to begin by thanking my wife, Shelley, who has provided support and encouragement throughout my pursuit of a Master's degree. My children, Claude and Carrie, have given me happiness and enthusiasm through their joy of discovering the world.

I would also like to thank Dr. Geerts, who has answered endless questions, performed countless experiments, and contributed many hours to helping me enjoy physics.

Thanks to the others on my thesis committee, Dr. Gutierrez and Dr. Spencer, and Dr. Anup, who have also helped me with patience and kindness.

This manuscript was submitted on April 19, 2002.

TABLE OF CONTENTS

	Page
LIST OF FIGURES	vii
LIST OF TABLES	x
ABSTRACT	xi
Chapter	
1 INTRODUCTION	1
1.1 Smallest Spot Size of the Laser Writer System	3
1.2 Hysteresis Curve	5
2 MEASURING THE PROPERTIES OF THIN FILMS	7
2.1 Optical Kerr Effect	7
2.2 Vibrating Sample Magnetometer	8
3 PHOTOLITHOGRAPHY EQUIPMENT AND CALIBRATION	10
3.1 Sputtering	10
3.2 Photoresist Chemistry	13
3.3 Hotplate	16
3.4 Spinner	16
3.5 Exposure	20
3.6 Visual Inspection of Patterned Photoresist and Thin Films	28
3.7 Etchant	35
4 LASERWRITER SYSTEM	36
4.1 Equipment	36
4.2 Auto-Focus Unit	38
4.3 Auto-Focus Setup and Calibration	40
4.4 Active Focusing Procedure	43
5 UNPATTERNED THIN FILM MEASUREMENTS	47
5.1 Etching Results	47
5.2 Estimated Deposition Rate	50
5.3 Hysteresis of an Unattached Thin Film	53
5.4 Hysteresis Loops of Various Film Thicknesses	56
5.5 Scanning Kerr Measurements	56
5.6 Coercivity vs. Film Thickness	63

6	PATTERNED THIN FILM MEASUREMENTS	67
	6.1 Stress Observed by the Stylus Profilometer	67
	6.2 Pattern Sizes Measured By Stylus Profilometer.....	69
	6.3 Hysteresis Curves of Patterned Thin Films	73
	6.4 Strain.....	76
	6.5 Demagnetizing Factor.....	77
	6.6 Domain Size	79
	6.7 Homogeneity of the Film Thickness over the Sample Surface.....	80
7	CONCLUSIONS	82
8	IDEAS FOR FURTHER RESEARCH.....	83
	8.1 Measuring Magnetic Hysteresis during Etching.....	83
	8.2 Effects of Stress on Patterned Thin Films	84
	8.3 Temperature Sensitivity Measurements.....	85
	8.4 Using the Laser Writer as a Profilometer.....	86
	8.5 Improving the Patterning Process	88
	8.6 Arrangements for Automated Scanning	88
	8.7 Creating Many Small Rectangular Patterns	89
Appendix A	Kerr and VSM Hysteresis Loops.....	91
Appendix B	Etch Series.....	94
Appendix C	Photolithography Procedure	98
Appendix D	Laser Writer Software Procedure	103
Appendix E	Laser Wavelength Selection	108
VITA	110
BIBLIOGRAPHY	111

LIST OF FIGURES

Figure 1-2 Etched NiFe Grating of Varying Pitch	4
Figure 1-3 Image of small structures written by laser writer. Scale is 1 micron per division.	5
Figure 1-4 Hysteresis Curve of a NiFe Thin Film.....	6
Figure 2-1 Vibrating sample magnetometer	8
Figure 3-1 EDX Analysis of NiFe 35% Sputtered onto Glass	12
Figure 3-2 EDX Analysis of NiFe 35% Sputtered onto Silicon	12
Figure 3-3 Novolak resin	13
Figure 3-4 Chemical process for photoresist. The resulting compound, indenecarboxylic acid, is soluble in developer.	14
Figure 3-5 AZ 5214-E Spectral Transmission (1.15 microns).....	15
Figure 3-6 Available output power of laser lines for 532 Argon Ion Laser	15
Figure 3-7 Measured thickness for a spin speed of 3,000 rpm.....	18
Figure 3-10 Exposure settings for patterns on sample #011130	21
Figure 3-13 Spot projected on equal sized photoresist pattern.....	24
Figure 3-14 Spot projected on larger sized photoresist pattern	25
Figure 3-15 Exposure test and calculated exposure values	26
Figure 3-16 Developed line and beam size for 116.6 mJ exposure	26
Figure 3-17 Developed line and beam size for 58.3 mJ exposure	27
Figure 3-18 Developed line and beam size for 23.3 mJ exposure	27
Figure 3-19 Developed line and beam size for 11.6 mJ exposure	27
Figure 3-20 Developed line and beam size for 5.8 mJ exposure	27
Figure 3-21 Developed line and beam size for 2.3 mJ exposure	28
Figure 3-22 Overexposed ends of line patterns	29
Figure 3-23 Underexposed line patterns.....	30
Figure 3-24 An etched line (dark pattern), and the alignment beam (light) used to create it. Aspect ratio is 10:1.	30
Figure 3-25 An etched line (dark) and alignment beam (bright) with aspect ration of 2:1.	31
Figure 3-26 Focus test patterns	31
Figure 3-27 Enlarged view of focus test pattern.....	32
Figure 3-28 Etched grating patterns of 12, 6 and 2 microns. 1 division is 1 micron.	33
Figure 3-29 Complete etch of a thin film	34
Figure 3-30 Incomplete etch of a thin film	34
Figure 4-2 Laser Writer Block Diagram	37
Figure 4-3 Optical path of the laser writer	38
Figure 4-4 Focused image	42
Figure 4-5 Unfocused images	43
Figure 4-6 Points used to calculate autofocus	44
Figure 5-1 Magnetization vs. etch time	48
Figure 5-3 Sputtering time vs. estimated thickness.....	52

Figure 5-4 Hysteresis loop of a NiFe 45% thin film as-sputtered.....	53
Figure 5-5 Hysteresis loops of both sides of the unattached thin film ...	54
Figure 5-6 Magnitudes of the coercivity of as-sputtered and unattached thin films	55
Figure 5-7 Kerr measurement for entire sample of NiFe on glass	57
Figure 5-8 Kerr measurement with spot size of .5 mm.....	58
Figure 5-9 Hysteresis curve of a Kerr measurement at the bottom edge of sample 10240104	58
Figure 5-10 Kerr hysteresis loop at the center of sample 10240104.....	59
Figure 5-11 Hysteresis loop of the bottom edge of sample 10260101 ...	59
Figure 5-12 Hysteresis loop of the center of sample 10260101	60
Figure 5-13 Hysteresis loop at the top edge of sample 10260101.....	60
Figure 5-14 Kerr measurement at 3 mm from bottom edge of sample 10260101	61
Figure 5-15 Kerr measurement at 3.5 mm from bottom edge of sample 10260101	61
Figure 5-16 Kerr measurement at 4 mm from bottom edge of sample 10260101	62
Figure 5-17 Kerr measurement at 4.5 mm from bottom edge of sample 10260101	62
Figure 5-18 Coercivity vs. film thickness	63
Figure 5-19 Coercivity vs. film thickness for NiFe 45%	64
Figure 5-20 Coercivity vs. thickness measured by VSM and Kerr	65
Figure 5-21 Coercivity vs. saturation magnetization	66
Figure 6-1 Scan of a Patterned Thin Film	67
Figure 6-2 Scan of Sample 102801-04	68
Figure 6-3 Scan of Sample 102701.....	68
Figure 6-4 Patterned Area where Thin Film Spontaneously Peeled Away	69
Figure 6-5 Profile of 5 micron wide lines.....	70
Figure 6-6 Profile of 1.55 micron wide lines.....	71
Figure 6-7 Profile of 0.9 micron wide lines.....	72
Figure 6-9 Sample 10250101, Unpatterned Area of Thin Film.....	73
Figure 6-10 Six Hysteresis curves from the Patterned Area of Sample 10250101	75
Figure 6-11 a) Isotropic distribution of domain orientations b) Effect of tension in the vertical direction.....	77
Figure 6-12 (a) Externally Applied Field Perpendicular to the grating; (b) Externally Applied Field Parallel to the grating. In the latter case there are no free poles and thus no demagnetizing field.	78
Figure 6-13 Film thickness measurements over a 1" silicon wafer	81
Figure 8-1 Configuration for Kerr measurements during etching.....	83
Figure 8-2	84
a) Side view of sample under applied stress b) Front view, perpendicular to grating c) Front view, parallel to grating.....	84
Figure 8-4 Gaps in the etched lines were created by the stepper motor	90

Figure C-1 A sample suspended in etchant. 101
Figure E-1 Example of photoluminescence 109

LIST OF TABLES

Table 1-1 Specifications for Mitutoyo Objectives.....	3
Table 3-8 Spin speed and thickness for AZ 5214-E photoresist	19
Table 3-9 Measured laser power through four objective lenses	21
Table 3-11 Computed energy for four objective lenses. Based on laser power of 70 mW, an aperture size of 20x20 steps, and a velocity of 4,000 steps/sec.	23
Table 3-12 Recommended settings for various objective lenses.....	24
Table 4-1 Specifications for the Mitutoyo M Plan lenses	37
Table 4-7 Sample curvature for various film thicknesses.....	45
Table 5-2 Estimated thickness from VSM measurements	51
Table 6-8 Profilometer Results of Patterned Thin Films	73
Table 8-3 Specifications for the APO SL 50x and 100x lenses.....	87
Table D-1 File listing for a procedure to etch grating patterns	105

ABSTRACT

FABRICATION AND MAGNETIC PROPERTIES OF PATTERNED THIN FILMS

by

Claude H. Garrett IV, B.S., M.S.

Southwest Texas State University

May 2002

Supervising Professor: Wilhelmus Geerts

Magnetic materials and their Magneto-Optical properties play a key role in today's technology. Research in this field can uncover new methods of recording digital data, or developing new types of force sensors.

The magnetic properties of thin films were examined using the Magneto-Optical Kerr Effect and a Vibrating Sample Magnetometer (VSM). Other properties were observed using spreading resistance measurements and null ellipsometry. Patterns on the thin films, stress, film thickness and orientation were observed to change the magnetic

properties. The magnetic coercivity (H_c) was used to gauge the changing magnetic properties of the thin films.

Thin NiFe-35% and NiFe-45% films were magnetron sputtered onto cleaned silicon and glass substrates. A laser beam writing system and photolithography techniques were used to etch large arrays of microstructures. The gross magnetic properties are then examined using a vibrating sample magnetometer. Detailed magnetic properties of the patterned films were examined using a Magneto-Optical Kerr Tracer. The Kerr rotation of the specular and first diffracted peak was measured as a function of the applied field. These results as well as the results of the influence of patterning on the magneto-elastic properties of the thin films are examined.

We can isolate the parameters of photolithography to demonstrate a stable process, and determine the smallest achievable pattern size with a laser beam writing system.

Furthermore, we have also examined how the magnetic properties of thin films change with various patterns, and examined the effects of the intrinsic stress of the thin film on its magnetic properties

CHAPTER 1

INTRODUCTION

The magnetic properties of granular or micro structured materials differ from those of continuous thin films. The magnetic reversal mechanism depends (among other things) on the size of the magnetic entities. Large magneto-elastic effects are to be expected if those entities approach the single domain limit that makes these systems interesting candidates in pressure, acceleration, and force sensors.

Force sensors have been created based on the stress dependence of the coercivity (H_c)¹.

Furthermore, data storage can be increased over conventional recording techniques by using ordered patterns of microstructures. An array of domain-sized structures has been used to record binary information at a higher density than with unpatterned thin films².

Small structures in a thin film are normally created by photolithographic procedures. The thin film is covered with a photosensitive layer, i.e. photoresist. In the exposure step certain areas

of the photoresist are exposed to light. In the development step, the exposed photoresist will be removed. This will create a mask for the final etching step.

At Southwest Texas State University, we have three different techniques to do the exposure.

Contact-printing in the microlab: A copy of the pattern to be created is printed on an overhead sheet. This overhead sheet is put in contact with the sample that is covered with photoresist. This sandwich is exposed with a lamp.

Optical microscope projection technique: The aperture of an optical microscope is removed and replaced by an overhead sheet that is printed with a copy of the pattern. The sample with the photoresist is placed under the microscope. The pattern on the overhead sheet is projected through the objective onto the sample.

Laser beam writer technique: A focused laser beam is used as a pencil and the pattern is directly written onto the photoresist by moving the sample with respect to the laser beam.

All structures created in this thesis were created with the laser beam writer. This system is described in Chapter 4 – Laserwriter System.

The structures created were grating patterns and rectangles of various dimensions. The gratings consist of parallel lines of 1mm in

length at a pitch of 4-10 microns. The rectangular patterns range in size of 10 microns down to less than 1 micron.

1.1 Smallest Spot Size of the Laser Writer System

The smallest attainable feature size is determined by the size of the focused laser beam and depends on the wavelength and the optics of the laser beam writer. The Rayleigh criterion relates those parameters with each other⁴:

$$d = \frac{0.61\lambda}{N_A}$$

Where d is the minimally resolved distance. The wavelength (λ) for the argon ion laser line used is 488 nm. The numerical aperture (N_A) for the 100x objective lens is 0.7, from Table 1-1.

	<i>APO SL 50X</i>	<i>APO SL 100X</i>
Numerical Aperture, NA	0.55	0.7
Working Distance, WD (mm)	13	6
Focal Length (mm)	4	2
Depth of Focus (microns)	0.9	0.6

Table 1-1 Specifications for Mitutoyo Objectives³

The smallest resolvable distance is then

$$\frac{0.61 \times 488nm}{0.7} = 425nm$$

There are variables in the process of creating structures that can greatly affect their size. These are development time, etch time, exposure and bake times. Also of importance in achieving the smallest possible structures consistently are temperature and humidity.

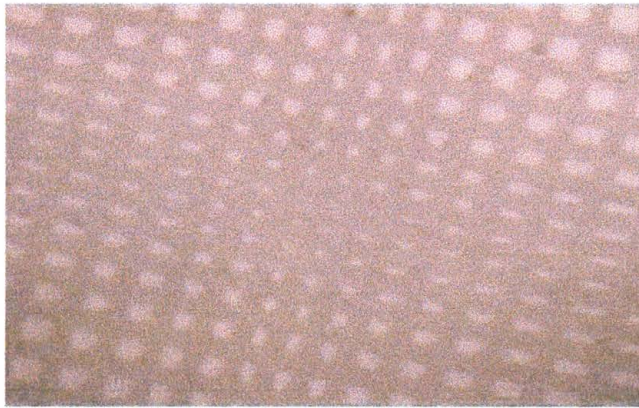


Figure 1-2 Etched NiFe Grating of Varying Pitch

Figure 1-2 shows a grating of varying pitch. By using this technique to create rectangles of various sizes, we have been able to produce thin film structures of less than 1 micron. We use a constant beam size, and start writing a grating pattern with a pitch of 5 microns along the x-axis. Then we reduce the pitch by 0.5 microns with each successive line written, down to a pitch that is equal to the beam size, leaving no space between the etched lines. Then the pitch is increased in the same way. The grating pattern is then repeated in the y direction.

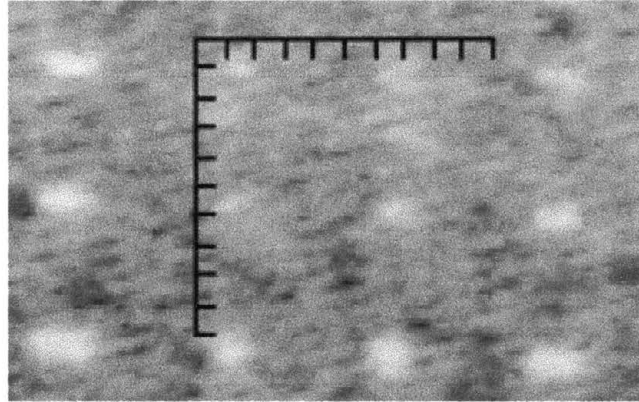


Figure 1-3 Image of small structures written by laser writer. Scale is 1 micron per division.

Taking a closer look at the center of this pattern (Figure 1-3), it can be seen that the smallest structures have dimensions of less than 1 micron. The following image was taken with red filters, so the resolution of the photograph is limited to about 800nm.

1.2 Hysteresis Curve

The magnetic characterization of the samples was done by a Vibrating Sample Magnetometer, and a Kerr tracer (See Chapter2). With both pieces of equipment it is possible to measure a magnetic hysteresis curve. Figure 1-4 is a graph that shows how the magnetic moment of a sample changes as a function of the applied magnetic field.

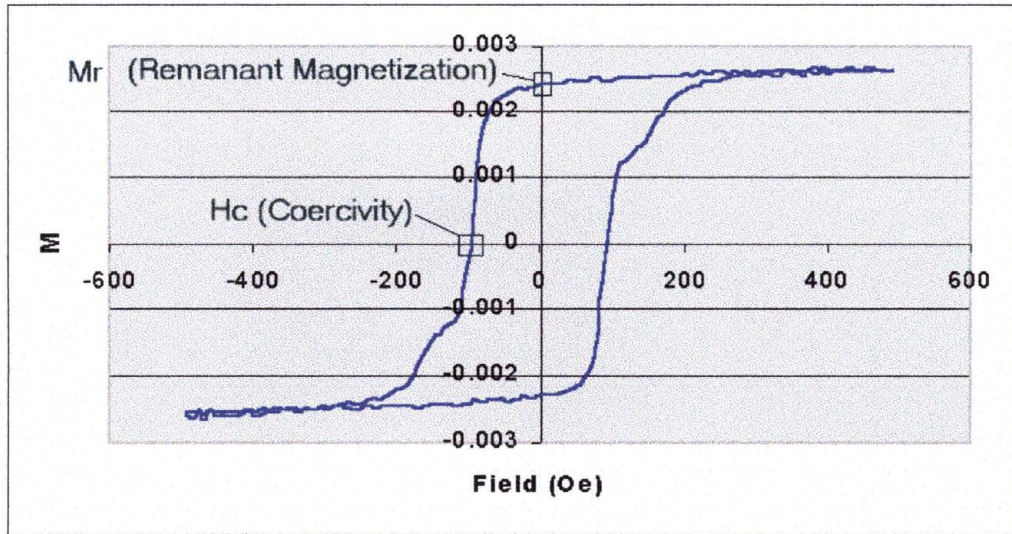


Figure 1-4 Hysteresis Curve of a NiFe Thin Film

The applied magnetic field is shown by the x coordinate. It increases from 0 to 500 Oe, and then is reduced to 0 Oe. The polarity is reversed (N and S poles are switched) to generate a negative applied field from 0 to -500 Oe, and back to zero again.

The response of the material is shown by the y coordinate. As the applied field increases, the material is magnetized. At the highest point of magnetization, the applied field has a diminishing effect (300-500 Oe). This is the saturation magnetization, M_s .

When the applied field is reduced to zero, the sample is still magnetized. This is the remanant magnetization, M_r .

The coercivity, H_c , is the applied external field that it takes to reduce the magnetization back to zero.

CHAPTER 2

MEASURING THE PROPERTIES OF THIN FILMS

2.1 Optical Kerr Effect

The Kerr effect can be used to measure the magnetization of a sample. A magnetic material has different reflection coefficients for right circularly polarized light and left circularly polarized light. The difference in the polarization of the incident and reflected beams is linearly proportional to the magnetization of the sample.

A laser of wavelength 632.8 nm is used as the light source. The penetration depth of visible light is typically 15-30 nm for metals. The spot size of the laser can also be adjusted. Thus the Kerr effect measurements are local to the surface and spot size of the laser for measuring the properties of the thin films.

Details of the Kerr equipment used in this project can be found in the thesis by Charles Watts⁴.

2.2 Vibrating Sample Magnetometer

In a vibrating sample magnetometer (VSM), a sample is suspended in a magnetic field and vibrated. The vibrating magnetic sample causes a flux change. This flux change induces a voltage in the pick-up coils, which are located on the surface of the pole pieces of the magnet. The flux, and therefore the induced voltage, is proportional to the magnetic moment of the sample.

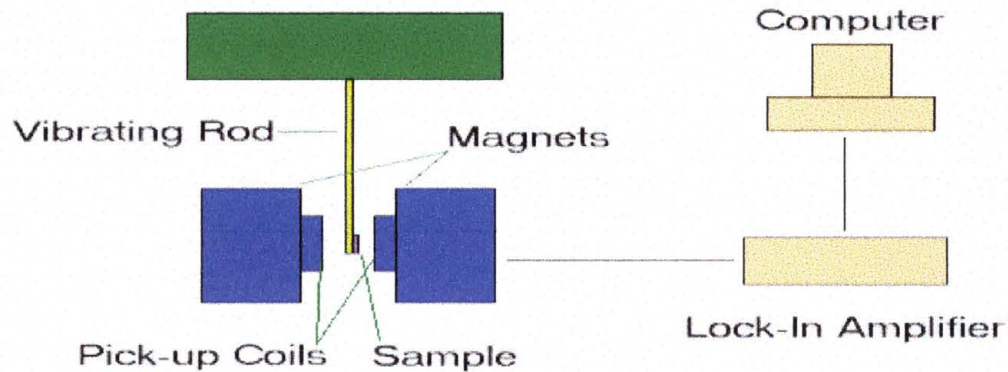


Figure 2-1 Vibrating sample magnetometer

When the sample is between the pickup coils, the magnetic induction is

$$\mathbf{B}_m = \mu_0(\mathbf{H} + \mathbf{M})$$

When the sample has moved away from the coils, the induction is

$$\mathbf{B}_0 = \mu_0 \mathbf{H}$$

And the change in induction is independent of H,

$$\Delta \mathbf{B} = \mu_0 \mathbf{M}$$

From Faraday's Law, the flux change induces an e.m.f. of

$$V = -NA \frac{dB}{dt}$$

or

$$\int V dt = -NA(B_f - B_i)$$

Which leads to

$$\int V dt = -NA\mu_0 M$$

and depends on M alone⁵. In reality the measurement is a little more complex, and not one pickup coil but eight pickup coils are used to measure the magnetization.

The signal from the pick-up coils is very weak. It is fed to a lock-in amplifier, along with the signal from the vibrating rod. The resulting magnetization measurement is plotted against the applied field to form a hysteresis loop.

CHAPTER 3

PHOTOLITHOGRAPHY EQUIPMENT AND CALIBRATION

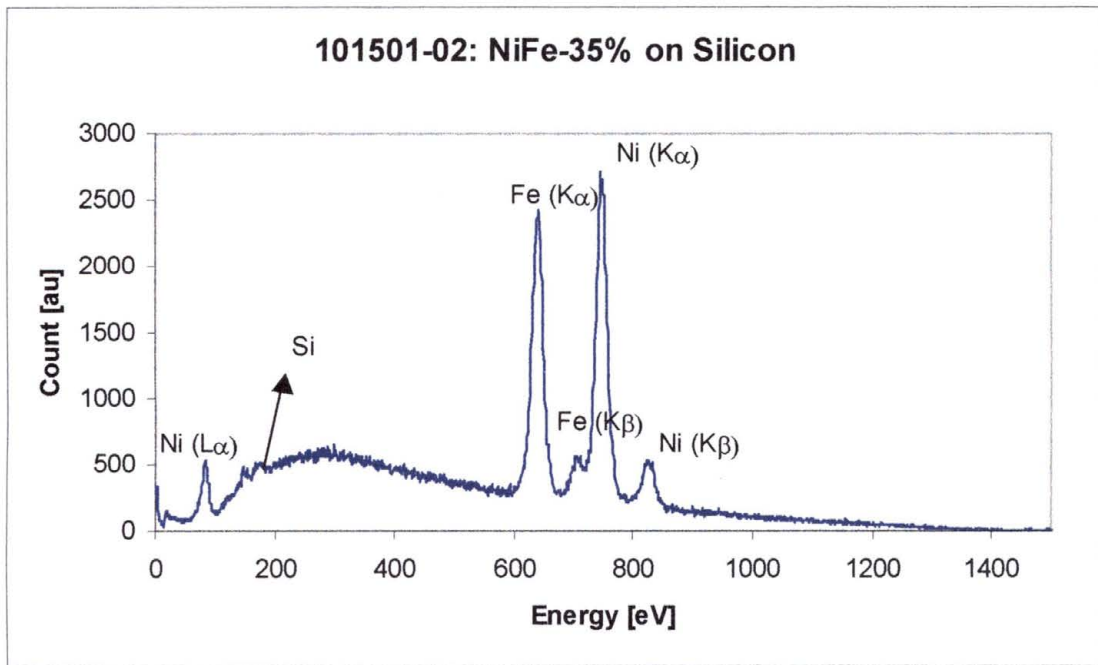
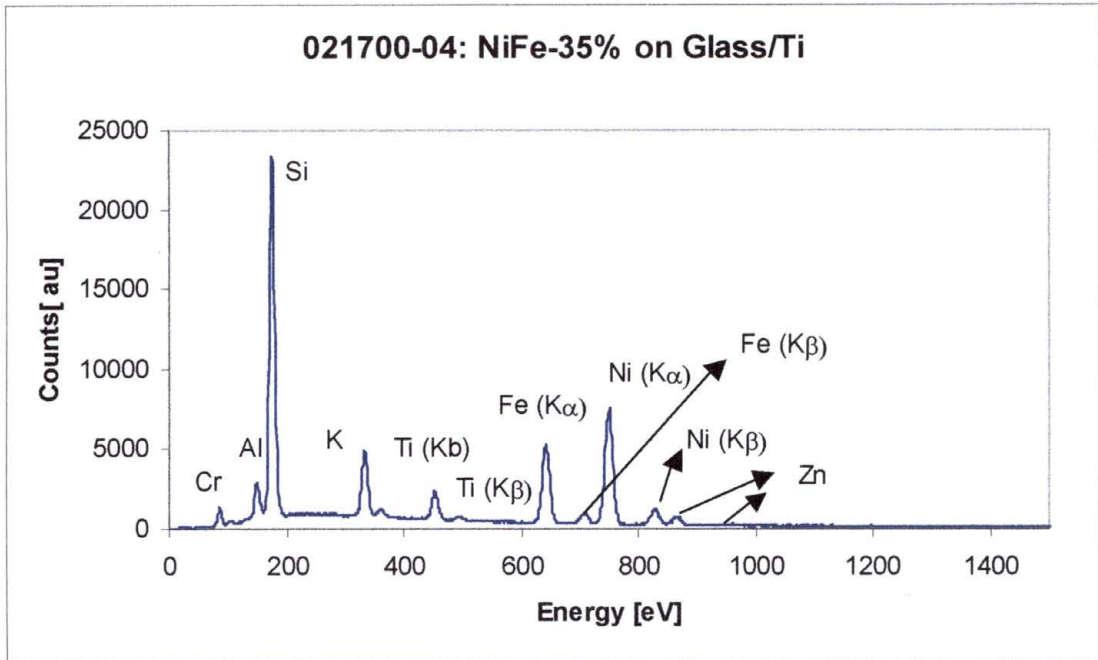
3.1 Sputtering

Thin films were created using DC Magnetron sputtering. The substrates used were glass and silicon. For glass substrates we used circular microscope cover glasses with a thickness of 0.2 mm and a diameter of 22 mm. Two types of silicon substrates were used. One inch wafers (thickness=0.3 mm, $\rho=1-20 \Omega \text{ cm}$, P-type, test-grade, (100) orientation, Wafer-World Inc.) and large pieces that were cut from 4-inch wafers (thickness=0.4 mm, $1-20 \Omega \text{ cm}$, P-type, test-grade, (100) orientation, Wafer-world Inc.). The silicon was covered with a native oxide layer. The glass substrates and 1" silicon wafers were cleaned ultrasonically in acetone and isopropyl alcohol. They were dried with nitrogen gas. The large silicon substrates were not cleaned before they were loaded in the vacuum system. All substrates were mounted in the vacuum system with small stainless blade springs. Two types of targets

were used: NiFe 35% and NiFe 45%. The original targets had a thickness of 1/8 inch. Because of flux-closure in the target-material, initially the guns would not light. We had to turn down the targets on our lathe. The working gas was Argon, with a background pressure of 8×10^{-7} Torr. Prior to sputtering, the substrates were subjected to a 350° C thermal flash. All samples were sputtered at a temperature below 50 °C. The power used for sputtering was 70 Watts. Films of different thicknesses were sputtered.

After sputtering, two samples were analyzed by EDX (Energy Dispersive Spectroscopy) analysis to determine their composition. The first sample we analyzed showed in addition to the expected Ni and Fe peaks significant quantities of Al, Si, Cr, K, and Zn. In particular we were concerned about the Zn, since this element is often a contamination of poorly maintained vacuum systems.

A more detailed analysis showed that the height of the peaks were strongly dependent on the used acceleration voltage and thus the probing depth of our EDX system. This suggested that the “contamination” was originating from the substrate. A quick search on the Internet indeed told us that the materials, including Zn, are typically used in the manufacturing of glass. Figure 3-1 shows the measured spectrum on sample 021700-04. The Ti peaks originate from a Ti cap layer and Ti seed layer. Figure 3-2 shows the spectrum of a sample sputtered on silicon.



There are no longer any strange peaks. We conclude from this analysis that our samples do not contain any measurable contamination. The percentage of iron in our samples sputtered with the NiFe-35% is approximately 31%. This is less than the iron percentage in the target. At the moment it is not clear why there is such a large difference.

3.2 Photoresist Chemistry

AZ 5214-E photoresist⁶ was used for the photolithography process. This is a positive resist, i.e. the exposed areas will be soluble in the developer. It is comprised of a Novolak resin (Figure 3-3) and naphthoquinone diazide as the photoactive compound. Upon exposure, the photoactive compound converts in the presence of water, to a base soluble chemical (See Figure 3-4 for process). 1 ml of photoresist was applied to each substrate during spinning.

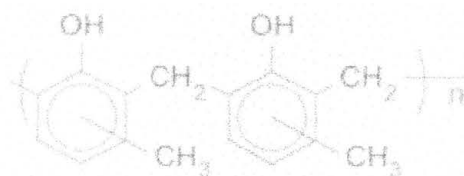


Figure 3-3 Novolak resin⁷

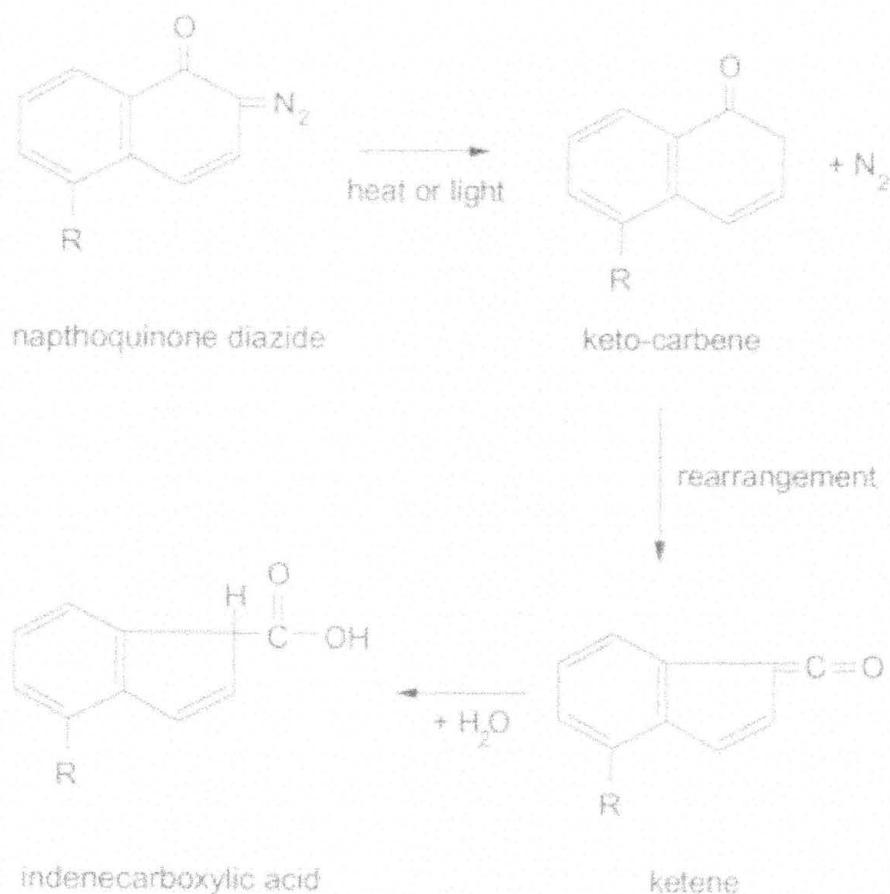


Figure 3-4 Chemical process for photoresist. The resulting compound, indenecarboxylic acid, is soluble in developer⁷.

AZ 400K developer⁸ was used to process the photoresist. It was diluted 1:4 with DI water.

Figure 3-5 shows a chart of the photoresist response curve. The photoresist is most responsive in the near UV (365-405 nm) and UV (300-350 nm) ranges. The AZ 5214-E data sheet shows that its spectral sensitivity interval is 310-420 nm (see appendix).

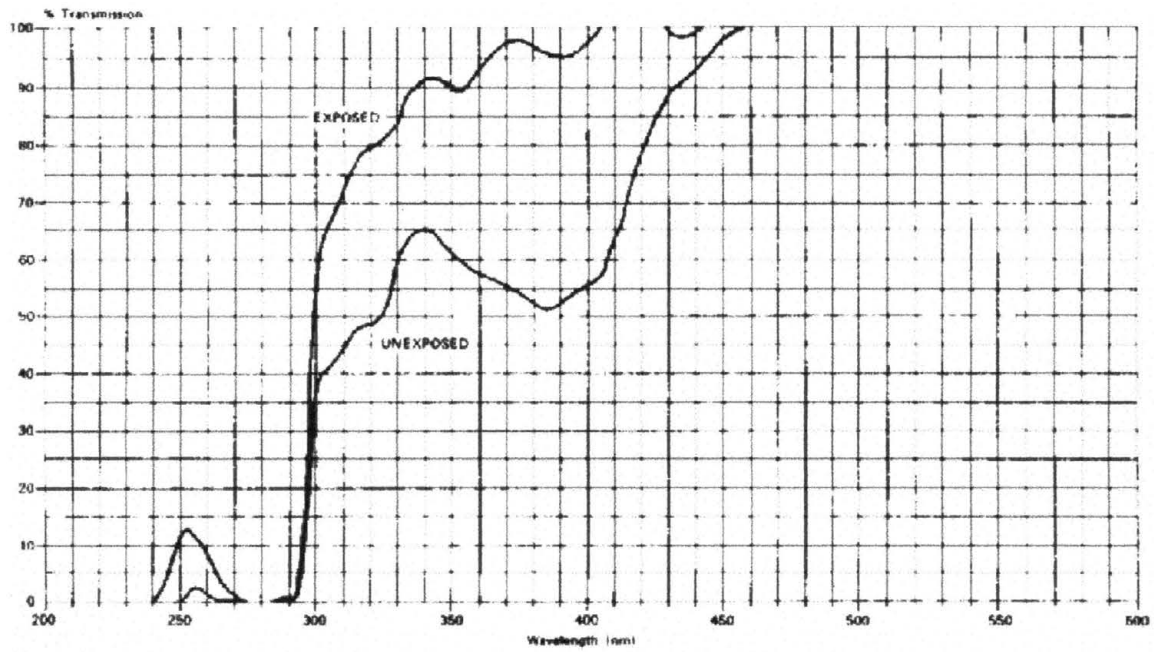


Figure 3-5 AZ 5214-E Spectral Transmission (1.15 microns)⁶

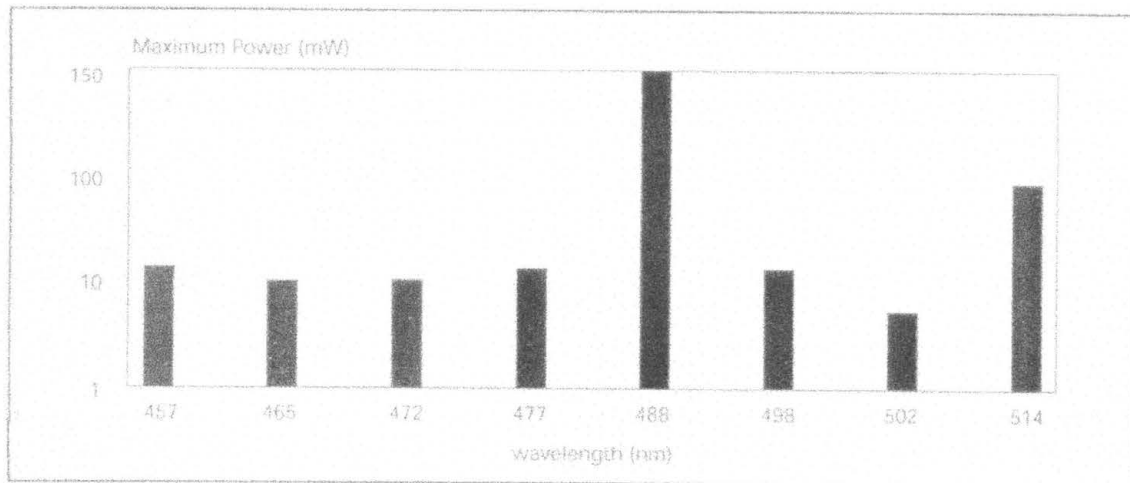


Figure 3-6 Available output power of laser lines for 532 Argon Ion Laser

Figure 3-6 shows the available laser lines. The deep blue laser line at 457 nm was chosen as the nearest to the response range of the photoresist. The selected line showed photoluminescence from the photoresist when the laser was writing to a sample coated with photoresist.

3.3 Hotplate

The hotplate is an EchoTherm Digital Hot Plate model HP30. A target temperature, timer and ramp rate can be set to control the heating.

3.4 Spinner

A Laurell Technologies Corp. WS-400A-6NPP-LITE spinner was used to distribute the photoresist. This spinner has options for setting the spin time, rotational velocity and acceleration. These settings can also be sequenced to create a programmed spin procedure.

The program used for spinning the photoresist on the thin films was a single step procedure. This was a spin for 30s at 3,000 rpm.

STEP 1: Duration 30s. Velocity: 3,000 rpm

Acceleration: 25 (2125 rpm/s)

An exhaust port is located on the back of the spinner, which vents into a chemical exhaust hood. A blower may be attached to the exhaust to increase the rate of air flow.

The spin speed and acceleration were adjusted by entering parameters into the spinner's control panel. The exhaust rate was adjusted by connecting a blower to the exhaust port.

There is a hole directly over the sample used to apply the photoresist. This hole is also an intake for air, which is drawn out through the exhaust port. Airflow exceeding the minimum specified was determined to disturb the homogeneous distribution of the photoresist.

To judge the photoresist thickness and consistency, we spun 4" silicon wafers and visually inspected the results. When adjusting the spinner settings, a speed of 3,000 rpm and an acceleration rate of 25 (2125 rpm/s) were determined to provide the most consistent results. For the exhaust rate, the lowest rate of airflow that met the minimum spinner specifications proved to be the best.

An eyedropper is used to apply the photoresist to the wafer through the hole in the lid over the sample. The photoresist is applied just before the spinner is started. As the wafer is spinning, the photoresist expands towards the edge of the wafer. Rings can be seen to expand from the center to the outer edge of the wafer. These are caused by an interference effect in the photoresist layer. While spinning, the thickness decreases. Depending on the thickness of the photoresist layer constructive or destructive interference will occur. After the spin is complete, the wafer can be examined for the uniformity of the photoresist. There should be 1-2 rings left on the wafer.

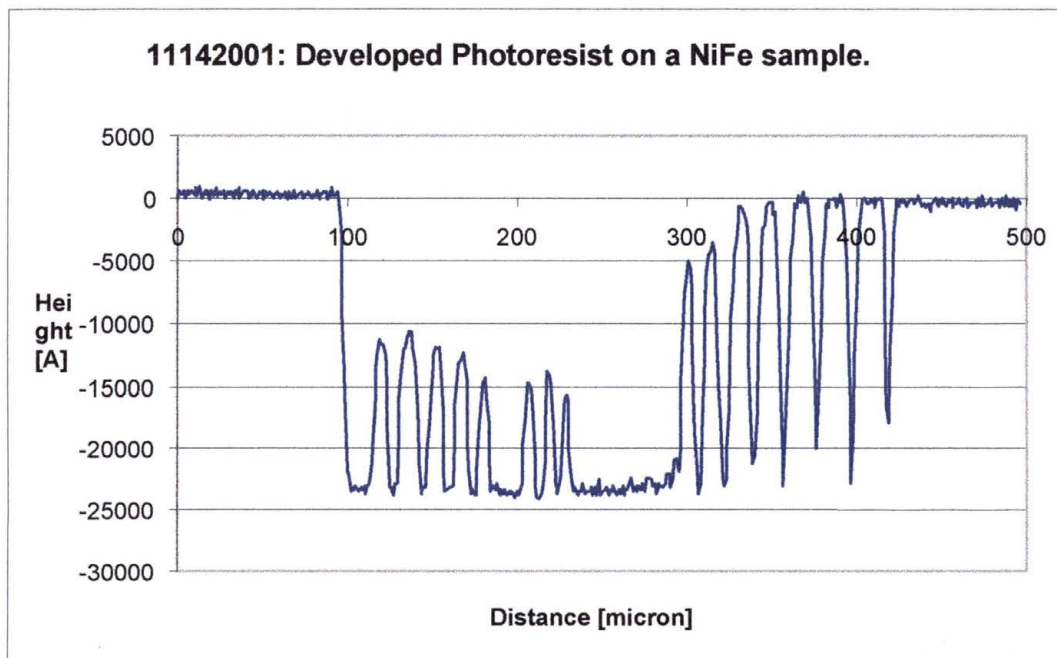


Figure 3-7 Measured thickness for a spin speed of 3,000 rpm

The thickness of developed photoresist was measured for sample 11142001 by the Tencor profilometer (Figure 3-7). This sample was

spun at 3,000 for 30s, after the application of 1 ml of AZ 5214-E photoresist. The thickness is 2.3 microns. We also notice that the photoresist does not have a uniform thickness. If the structures become small, the photoresist on top of the structures becomes thinner. We believe that this is due to reflections from the thin film and focusing problems. The depth of focus of the laser beam writer is 0.6 microns which is considerably thinner than the thickness of the photoresist. For better results we can recommend selecting a photoresist with a lower viscosity so that thinner layers can be spun.

Spin Speed (rpm)	Thickness (microns)
3000	1.63
4000	1.41
5000	1.26
6000	1.15
7000	1.01

Table 3-8 Spin speed and thickness for AZ 5214-E photoresist

From Table 3-8, the estimated thickness should be 1.63 microns, as opposed to 2.3 microns as measured by the profilometer. A search on the internet revealed that other institutes found a discrepancy between the measured spin speed thickness relation and that provided on the data sheets of the manufacturer.

The Mechanical Engineering department of the University of Maryland⁹ found a thickness of 2.5 microns for a spin speed of 4000

rpm. Although it is not clear why there is such a large difference, evaporation of part of the solvent and thus an increase in the viscosity of the photoresist are plausible explanations.

3.5 Exposure

Exposure of the photoresist depends on many factors. These include film thickness, soft bake conditions, spectral output of the laser, and development conditions¹⁰. Development conditions include the developer type, dilution, duration, agitation, temperature and humidity.

Since exposure and development are interrelated, a baseline for developing was used, and the exposure adjusted from there. The basic developing procedure uses AZ 400K developer, diluted 1:4 with DI water developed at room temperature (25° C) for 60s with agitation of 1 rpm.

The laser power was measured at the objective lens of the microscope. The measurements were made for the most powerful peak of the laser (the green line) at 488 nm. The laser power was set at the control panel to 100 mW.

Table 3-9 shows the laser power measurements made with a Metrologic Photometer.

<i>Lens</i>	<i>Laser Power</i>	<i>Aperture</i>	<i>Green Line Power (mW)</i>
5x	100 mW	20	0.09
20x	100 mW	20	0.085
50x	100 mW	20	0.075
100x	100 mW	20	0.01

Table 3-9 Measured laser power through four objective lenses

The throughput of the 100x objective is considerably less than the other objectives. At this moment it is not clear why.

The blue line was used to expose the photoresist. The ratio of green to blue is ~ 15:1 (wavelength 488 vs. 457 for model 532 argon ion lasers).

Sample 011130 was used to test exposure and development. It consists of a thin Al film on silicon. After coating with photoresist, it had line patterns exposed at levels indicated by Figure 3-10.

<i>Laser Power (mW)</i>	<i>Aperture steps (.1 microns/step)</i>	<i>Velocity (steps/second)</i>
140 mW	20x20	2000
70 mW	20x20	2000
70 mW	20x20	4000

Figure 3-10 Exposure settings for patterns on sample #011130

The exposure level is the highest for the first pattern (140 mW at a velocity of 2000 steps/sec). The next pattern was exposed at half the power (70 mW at 2000 steps/sec.). The third pattern was exposed at twice the velocity as the second, reducing the exposure to ¼ of the first pattern (70 mW at 4000 steps/sec.).

The optimal energy to expose the photoresist is in the range of 25-75 mJ/cm², based on the specifications for AZ 5214-E photoresist¹¹. We can check that this is what was delivered to create the pattern that appears to be exposed and developed correctly. It could be the case that the photoresist was overexposed and underdeveloped, or the other way around. This would be discovered by determining the energy delivered to the photoresist.

The measured green line power of the 100x lens at an aperture of 20x20 with a laser power of 100 mW is .01 mW. We use the purple line to expose photoresist. The ratio of green to purple is ~ 15:1 (wavelength 488 vs. 457 for model 532 argon ion lasers). This gives a blue line power of $6.66 \cdot 10^{-7}$ W.

The velocity used to draw the line was 4,000 steps/s. The spot size was 20 steps wide. This gives an exposure time of 0.005 sec.

$$\frac{20 \text{ steps}}{4,000 \text{ steps / sec}} = 0.005 \text{ sec} .$$

For the 100x objective lens, the area is .1 steps/micron. For a spot size of 20x20, this would be 2x2 microns, or a total area of $4 \cdot 10^{-12}$ m².

The laser was set at 70 mW to draw the line, instead of 100 mW when the power was measured through the lens. This gives a power of 70% of the blue line power. $70\% * 6.66 * 10^{-7} \text{ W} = 4.66 * 10^{-7} \text{ W}$.

The energy delivered to the photoresist through the 100x lens is then

$$\frac{4.66 * 10^{-7} \text{ W} * 0.005 \text{ sec}}{4 * 10^{-12} \text{ m}^2} = 583.33 \text{ joules / m}^2$$

Or 58.33 mJ/cm². This is in the range of 25-75 mJ/cm².

This computation was performed for each lens (Table 3-11).

Lens	Green Line Power (W)	Blue Line Power (W)	Exposure Time (s)	area (m ²)	Power (W)	Energy (mJ/cm ²)
5	0.00009	0.000006	0.01	1.6E-09	0.0000084	1.31
20	0.000085	5.66E-06	0.01	1E-10	7.933E-06	19.83
50	0.000075	0.000005	0.01	1.6E-11	0.000007	109.37
100	0.00001	6.66E-07	0.005	4E-12	4.667E-07	58.33

Table 3-11 Computed energy for four objective lenses. Based on laser power of 70 mW, an aperture size of 20x20 steps, and a velocity of 4,000 steps/sec.

With the lower magnifications it is possible to draw wider lines. From Table 3-11 we can also conclude that the highest speeds can be obtained with a 50x objective. Table 3-12 gives the recommended speed and power for the different objectives for the case that the aperture is set to 20x20 steps.

<i>Lens</i>	<i>Laser Power</i>	<i>Recommended Velocity (steps/sec)</i>	<i>Energy (mJ/cm²)</i>	<i>Aperture (steps)</i>	<i>Line Width (microns)</i>
5	70	90	58.33	20	20
20	70	1300	61.02	20	10
50	70	8000	54.69	20	4
100	70	4000	58.33	20	2

Table 3-12 Recommended settings for various objective lenses.

After development, sample 011130 was placed back into the laser writer. The spot size was set to the same size that was used to draw the lines. A correct exposure level and development will yield lines that are as wide as the spot that was used to create them, as Figure 3-13 shows from the third pattern created.

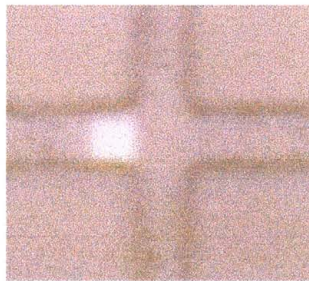


Figure 3-13 Spot projected on equal sized photoresist pattern

Figure 3-14 shows that an overexposure, as in the case of the first two patterns, will show lines that are wider than the spot size.



Figure 3-14 Spot projected on larger sized photoresist pattern

Sample 011130 (aluminum on silicon substrate) was patterned with an exposure test pattern. This is a series of lines at varying speeds to find the best exposure level for a given aperture size. The exposure test pattern was written onto each sample to verify the stability of the exposure and development process through time.

Figure 3-15 shows such an exposure test pattern. On the right side of the figure the exposure dose is listed. This pattern was created from right to left, line by line. There are three groups of six lines each.



mJ/cm^2
116.6
58.3
23.3
11.7
5.8
2.3
116.7
58.3
23.3
11.7
5.8
2.3
2333.3
1166.7
466.7
233.3
116.7
46.7

Figure 3-15 Exposure test and calculated exposure values

Figures 3-16 through 3-21 show enlarged views of the first exposure pattern (top six lines in Figure 3-15).

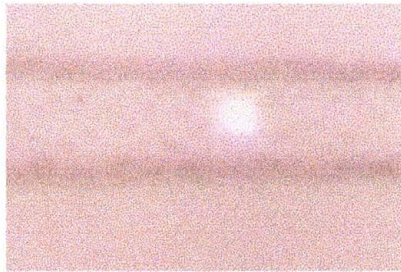


Figure 3-16 Developed line and beam size for 116.6 mJ exposure

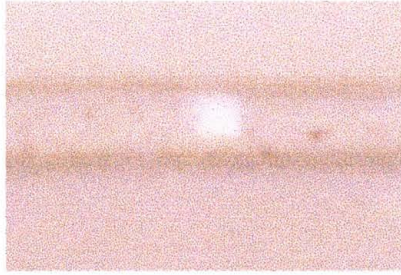


Figure 3-17 Developed line and beam size for 58.3 mJ exposure

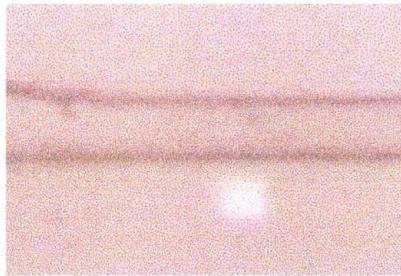


Figure 3-18 Developed line and beam size for 23.3 mJ exposure

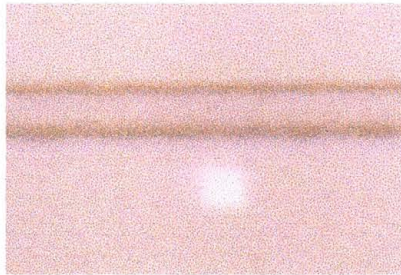


Figure 3-19 Developed line and beam size for 11.6 mJ exposure



Figure 3-20 Developed line and beam size for 5.8 mJ exposure



Figure 3-21 Developed line and beam size for 2.3 mJ exposure

From figures 3-16 through 3-21, 3-19 shows the thinnest possible line without interruption, exposed at 11.6 mJ. However, to etch consistent patterns, figure 3-18 should be considered, with an exposure of 23.3 mJ. This is due to variations in the photoresist over the surface of the sample. Also, if the same exposure was used on the same sample, and development repeated, the development time would have to be changed to produce the same results. This is due to the changes in the unexposed photoresist that occur in the developer.

3.6 Visual Inspection of Patterned Photoresist and Thin Films

Figure 3-22 shows that the endpoints of the lines in the vertical direction are flared. This is due to the fact that there is a delay while the

platter accelerates and decelerates. The lines were drawn in alternating directions of up and down.

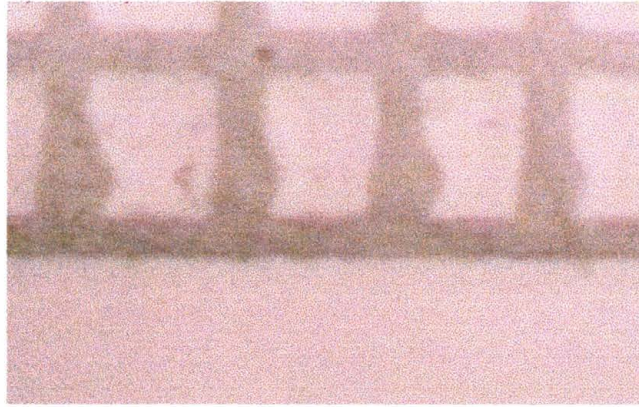


Figure 3-22 Overexposed ends of line patterns

Figure 3-23 shows regular breaks in the lines. These are due to the fact that stepping motors are used to control the platter in the x and y direction. By changing the spot size from a square to a rectangle, with the same y dimension, but longer in the x direction, the lines can be smoothed out, and the exposure time reduced

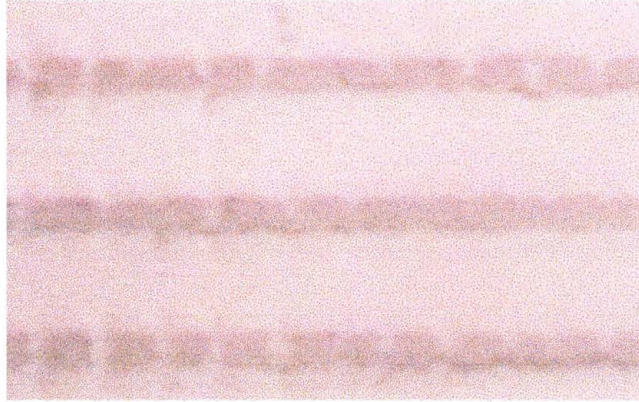


Figure 3-23 Underexposed line patterns

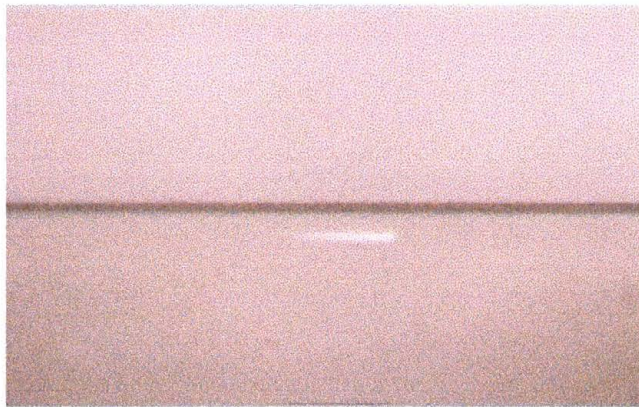


Figure 3-24 An etched line (dark pattern), and the alignment beam (light) used to create it. Aspect ratio is 10:1.

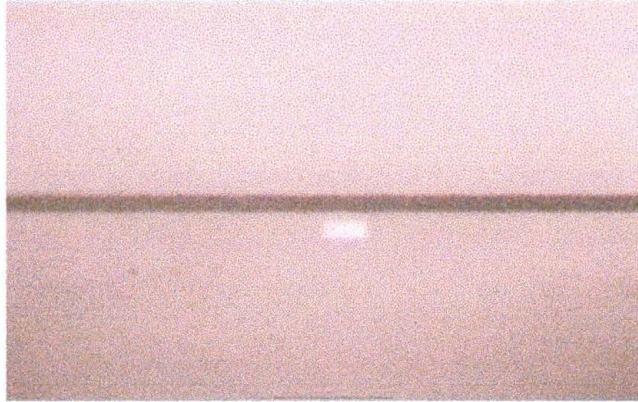


Figure 3-25 An etched line (dark) and alignment beam (bright) with aspect ratio of 2:1.

Figures 3-24 and 3-25 show that by using an aspect ratio of 10:1 and 2:1 creates smoother lines.

Figure 3-26 shows a series of patterns to test the focus of the laser. Since the optics of the microscope for the eyepieces may not be in focus with the CCD camera, and also the fact that the camera focuses using red light and the laser wavelength is selected at the blue end of the spectrum, the system may not be in relative focused. That is, when the alignment beam is in focus, the laser may be out of focus.

Each group consists of nine lines. The longest line in the center of each pattern is focused at a relative z coordinate of 0. The lines above are at -5, -10, -15 etc. and the lines below are at +5, +10, +15 etc. Each of the 8 patterns is also shifted in focus relative to the others.

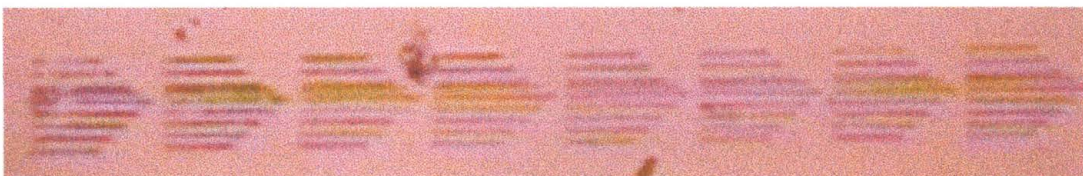


Figure 3-26 Focus test patterns

A close-up image of one of the focusing groups at the center of the entire pattern shows that the desired focus is at the longest line or just below (Figure 3-27). The top line appears to have disintegrated due to being out of focus.

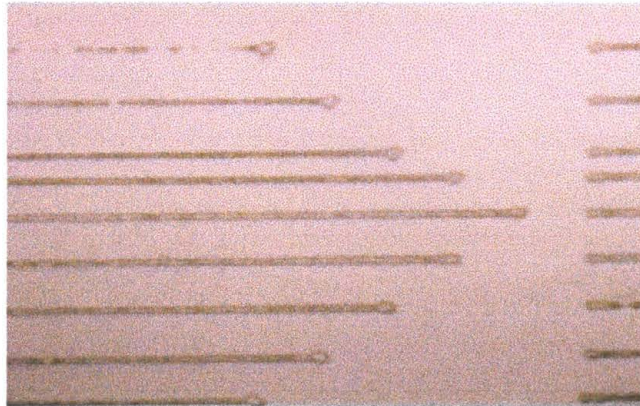


Figure 3-27 Enlarged view of focus test pattern

After optimizing the photolithography steps we used a diluted Aluminum etchant to copy the pattern in the photoresist into the thin NiFe film.

The wet etch process is isotropic in nature, and causes undercutting and imposes limits on the aspect ratio. The aluminum etch process occurs in two steps. In the first step, nitric acid oxidizes the aluminum to Al_2O_3 . In the second step, the Al_2O_3 is dissolved in the phosphoric acid. The water and acetic acid behave only as diluents. We assume that the etching of the NiFe films follows a similar mechanism.

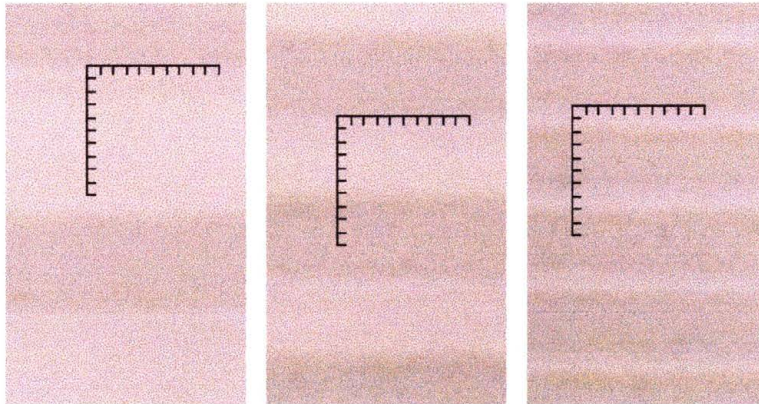


Figure 3-28 Etched grating patterns of 12, 6 and 2 microns. 1 division is 1 micron.

Figure 3-28 shows large, medium and small grating patterns etched in NiFe.

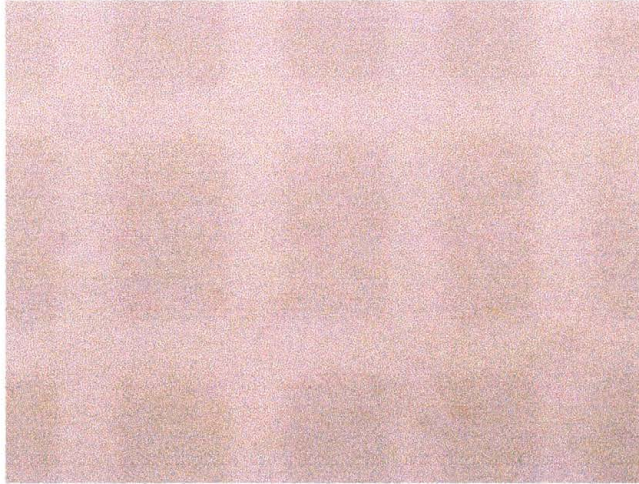


Figure 3-29 Complete etch of a thin film

Figure 3-29 shows dark rectangles of the thin film (of various sizes), after a complete etch. The laser writer created the light colored lines through photolithography. The beam size was constant. This sample is etched down to the silicon substrate, which is indicated by the light color of the lines between the rectangles.

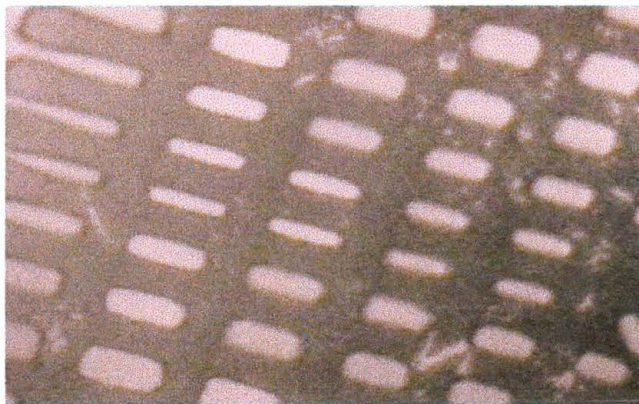


Figure 3-30 Incomplete etch of a thin film

Figure 3-30 shows an incomplete etch of the thin film. The film turns dark during the last stage of etching. This is due to the thickness of the thin film being less than the optical penetration depth. To the left of the image where the dark bands are a lighter shade of gray, the etching is more complete, but not down to silicon yet. The bright flakes of metal on the dark bands also indicate that etching is not complete.

3.7 Etchant

The etchant is an Al etchant that is diluted 1:3 with H₂O at room temperature. The resulting composition is¹²

27 vol% phosphoric acid H₃PO₄ (85%)

2 vol% nitric acid HNO₃ (100%)

2 vol% Acetic acid CH₃COOH (100%)

69 vol% H₂O

CHAPTER 4

LASERWRITER SYSTEM

4.1 Equipment

The laserwriter system is a Florod Corporation model LDS. It consists of an Argon Ion 500 mW laser model 532. The laser is switched on and off by an electromechanical shutter that is controlled by a computer. Its active wavelength is adjusted by an Oriel linear variable interference filter. The selected wavelength then proceeds into a microscope to be focused on a sample. An alignment beam from a quartz halogen lamp is filtered and focused coincidentally with the laser beam. Both the laser and the alignment beam pass through variable shutters that make up an aperture. The shutters are adjustable in the x and y directions. This is used to select the beam size and shape.

For the finest detail, a Mitutoyo M Plan APO 100x objective lens is used. Table 4-1 shows that the 100x objective lens has a numerical aperture of 0.7.

	<i>APO SL 50X</i>	<i>APO SL 100X</i>
Numerical Aperture, NA	0.55	0.7
Working Distance, WD (mm)	13	6
Focal Length (mm)	4	2
Depth of Focus (microns)	0.9	0.6

Table 4-1 Specifications for the Mitutoyo M Plan lenses

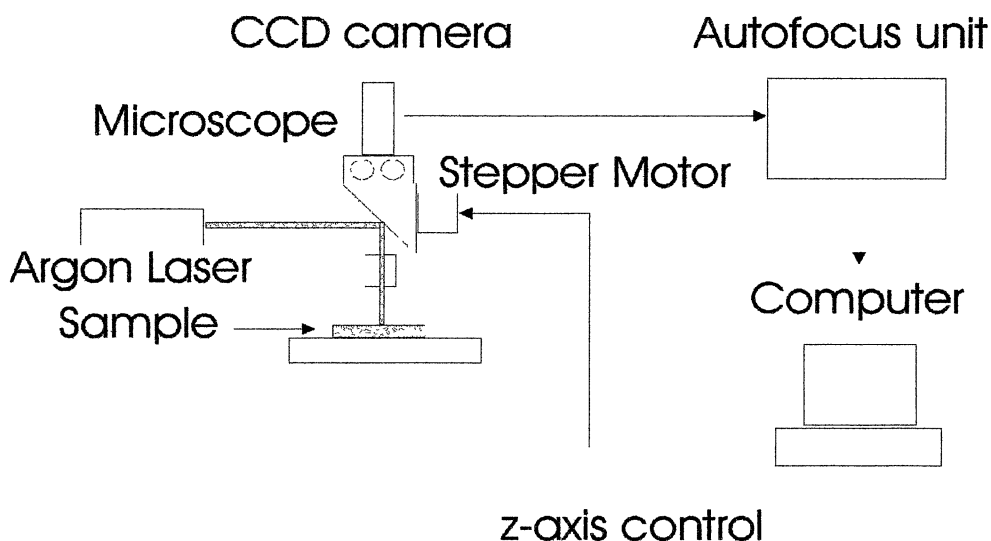


Figure 4-2 Laser Writer Block Diagram

Figure 4-2 shows a block diagram of the laser writer. The platter that the sample sits on controls the beam position on the sample. This platter can be moved by computer controlled stepper motors to an accuracy of 40 steps per micron in the x and y directions.

The intensity of the beam can be controlled manually by adjusting the laser power supply controls. The intensity can be adjusted from 30 to 500 mW.

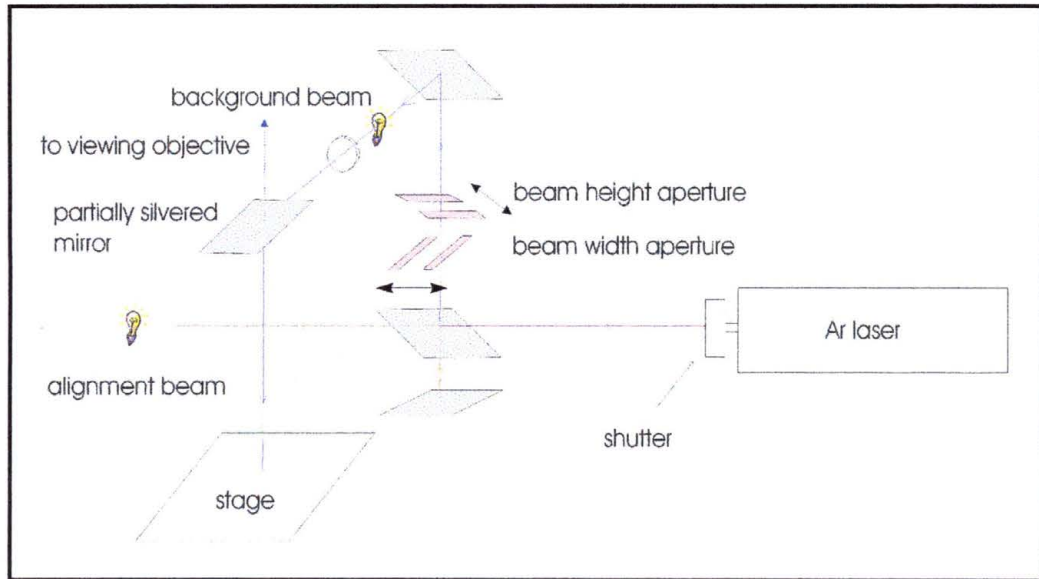


Figure 4-3 Optical path of the laser writer

Figure 4-3 shows the optical path of the laser writer. A CM-730 Y/C CCD camera is mounted on top of the microscope assembly. This provides a video signal to a monitor for viewing the sample in addition to the eyepieces. The video signal is also routed to a Prior Scientific ProScan autofocus unit. The autofocus unit is also computer controlled, and focuses the microscope by using a stepper motor that is affixed to the fine focus knob.

4.2 Auto-Focus Unit

When creating parallel lines 1mm long for gratings, it was discovered that the laser writer system would not stay in focus. This was

due to the sample not being flat, the x-y table not being flat, and due to mechanical drift in the setup.

The auto-focus system was installed and linked to an IBM PC computer. It is connected to the COM1 serial port of the computer. The autofocus unit also controls a stepper motor, which is connected to the focus knob of the laser writer system.

The CCD camera was installed using a screw-type mount, and rotated until the camera image was in focus with the optical image through the microscope eyepieces. The video signal runs directly into the autofocus unit.

The autofocus system uses the video signal as a guide to focus the image, and activates the stepper motor to control the focus knob until the video signal is in focus.

The autofocus system samples the video signal, and determines from its contrast the relative focus of the image (it's "focus score"). This is expressed as an integer. A very sharp image will have a higher focus score than a blurry image. The auto-focus unit determines the focus score by the image's contrast, and the focus score can be relayed to the computer.

The autofocus unit can also be sent a command from the computer to adjust the focus knob (by the stepper motor) until the best quality of focused image is obtained (by the video signal). This is the autofocus command.

To ensure that the beam remains in focus for very long line segments, the focus can be adjusted automatically. However, the focus has to also be adjusted dynamically. This is because the autofocus command takes the microscope out of focus to adjust the video signal to the best-focused position. Therefore, it cannot be used when a line is actually being drawn. Also, stopping periodically to focus and then continuing with the same line will produce exposure differences within the line segment. This is due to the delay in acceleration of the platter with respect to the electromechanical shutter that switches the laser on and off.

This can be remedied by updating the focus by using calculated values from the computer. These values are based on focusing information taken prior to drawing a pattern with the laser writer.

4.3 Auto-Focus Setup and Calibration

The Video port from the CCD camera is connected to the VIDEO-IN port of the auto-focus unit. The VIDEO-OUT port of the auto-focus unit is connected to a Sony Trinitron PVM 14N6U video monitor. The Z output from the auto-focus unit is connected to the stepper motor. This stepper motor is attached to the focus knob of the microscope. The RS232-1 port of the auto-focus unit is connected to the COM1 port of an IBM compatible AMD-K7 processor based computer with 128 MB RAM.

Once all of the hardware connections are established, tests can be performed to ensure that the auto-focus unit is operating correctly and that it is communicating with the host computer.

To test the hardware, ensure that the controller knob adjusts the focus via the stepper motor. The focus should be smooth, and the knob should not slip while being adjusted. The stepper motor should also not be so tight against the knob that it binds and cannot turn easily.

The software tests can be initiated by sending commands to the auto-focus unit by a terminal program on the computer. To run the terminal program, look on the desktop and open the folder “new stepmotor code”. Then run the program TTY.exe. Choose Settings from the menu, and check the boxes for “New Line” and “Local Echo”. Then click the OK button. Under the Action menu choose Connect.

Now the auto-focus unit should be ready to receive commands from the computer. Type in a “?” (without the quotes) and press Enter, and configuration information should be returned from the auto-focus unit starting with the line PROSCAN INFORMATION. If there is no response, try the command again and watch the TX and RX lights on the auto-focus unit. When a character is sent (the “?” or the Enter key pressed), the RX light should blink. When information is being sent to the computer, the TX light should blink also.

For the next step, adjust the alignment beam (knob B) on the laser writer to maximum intensity, and the background illumination (knob A) to minimum intensity. Set the shutters to a size of 80x80.

Focus the square and enter the command "FS" in the terminal program. The auto-focus unit should return an integer. This is the focus score. The command can be issued several times, and a different focus score may be returned each time. For the Figure 4-4, the focus score returned was between 190 and 235 for five iterations. An average that is above 100 is focused well.

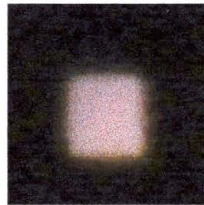


Figure 4-4 Focused image

If the auto-focus unit consistently returns 0, the SHUTTER screw on the side of the CCD camera may need to be adjusted with a small screwdriver.

Now, turn the focusing knob until the image is slightly out of focus.

The images in Figure 4-5 returned a focus score of zero.

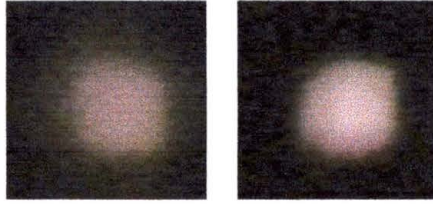


Figure 4-5 Unfocused images

Now enter the command “A” and press Enter. This will initiate an auto-focus procedure. The image on the monitor should flash and come back into focus.

4.4 Active Focusing Procedure

To correct the focus while the laser writer is exposing a pattern, the computer will request the x and y coordinates from the laser writer. The correct focus can then be computed and sent to the auto-focus unit.

The computer calibrates the auto-focus for each sample through a software procedure. The procedure measures the focus at 4 corner points on a 1mm bounding box. This is a box that is 1mm on each side, and encloses the pattern to be drawn by the laser writer (Figure 4-6).

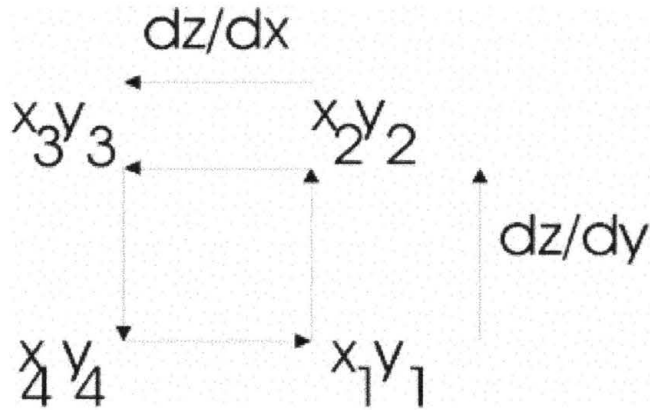


Figure 4-6 Points used to calculate autofocus

A command to move to each of the four points is issued to the laser writer. Then the autofocus command is sent to the autofocus unit. After the focus is performed, the z coordinate is requested from the autofocus unit. The four sets of (x,y,z) coordinates (one for each point) are saved. The values of dz/dx and dz/dy are computed through linear interpolation.

$$\frac{dz}{dy} = \frac{z_2 - z_1}{y_2 - y_1} \qquad \frac{dz}{dx} = \frac{z_3 - z_2}{x_3 - x_2}$$

Once dz/dx and dz/dy are computed, the image may be focused at any point, and at any time, even when the laser writer is actively drawing a pattern.

For example, as the laser writer is drawing a line, the x and y coordinates are requested by the computer. The z coordinated is computed for optimal focus, and the resulting z coordinate is sent to the autofocus unit. Because of the limited speed of the serial connection to the autofocus unit (9600 baud), this happens at 4-5 times per second.

This is adequate for the scanning speeds we use at the selected laser intensity (currently up to 4000 steps/sec.).

The resulting patterns that have been generated with the new autofocus are much more homogeneous than those that were made in the past. The linear interpolation algorithm does not correct for the bending of the samples. Most of the samples, in particular the thicker films, are thicker because of the inherent stress created during deposition. Table 4-7 shows the curvature of some of the NiFe samples on silicon as a function of film thickness.

<i>Sample Name</i>	<i>Thickness (nm)</i>	<i>Depth of the cup (Angstroms)</i>
Silicon	NA	3500
102801-01	10.53	2300
102801-02	93.76	3600
102701-01	288.3	Peeled off substrate during etching
102701-04	397.5	4000
102701-03	577.5	8000
102701-02	803.4	8800
102701-02	1296	Peeled off substrate during etching

Table 4-7 Sample curvature for various film thicknesses

The measured curvature over 5 mm for films under 400 nm is of the same order of magnitude (400 nm) as the depth of focus of the 100x objective lens (600 nm). So for a 1x1 mm square pattern the linear interpolation is sufficient to adjust the focus.

Problems are to be expected for the thicker films and the films on glass microscope slides that show considerably more curvature (up to 0.88 microns).

CHAPTER 5

UNPATTERNED THIN FILM MEASUREMENTS

5.1 Etching Results

To determine the etch rate, samples were etched at intervals, and the coercivity plotted against time.

The VSM was used to measure the bulk magnetic properties of the samples in the form of hysteresis curves. The hysteresis curve was measured immediately after each etching, to reduce the time for an oxide layer to form on the etched NiFe surface. From the hysteresis curve, the coercivity was plotted against time to reveal the etch rate.

Each sample was glued to the plastic rod of the VSM. They were placed in a solution of diluted Aluminum etch (See Chapter 3 – Chemistry).

135nm NiFe 35%

An NiFe 35% film on a silicon substrate was glued to the plastic rod of the VSM. It was placed into the VSM and measured. The initial

magnetic moment was 8.79×10^{-3} emu. After this, the sample was etched for 15 seconds at a time, and the measurements repeated until the magnetization was 2.29×10^{-5} emu.

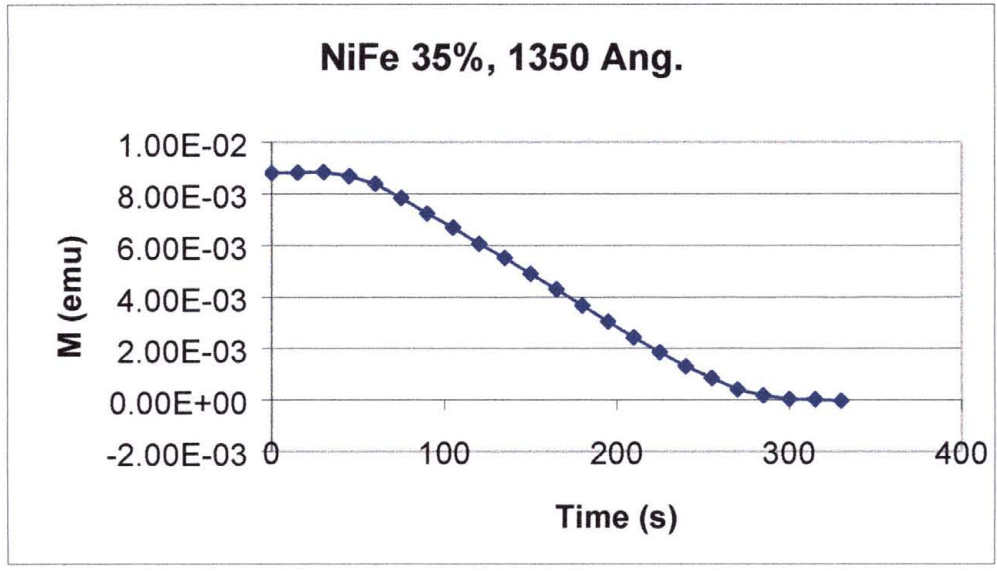


Figure 5-1 Magnetization vs. etch time

Figure 5-1 shows the results of the etch time vs. coercivity.

The etching takes about 30 seconds to begin, and after 45 seconds proceeds at a roughly linear rate of 5.6 Å per second.

It is believed that the metal oxide layer causes the initial delay in etching. The thickness of the natural oxide on Ni is approximately 10 \AA^{13} . The etch rate slows at the endpoint as it reaches the silicon.

During etching, it was noticed that the NiFe film turns dark brown during the last 30 seconds. This endpoint detection scheme was later used to etch patterned samples. Assuming that the etch rate does not change for the last part of the film, 30 seconds corresponds to

approximately 15 nm. This is thinner than the penetration depth of the light which explains the different color.

600nm NiFe 31%

A nickel iron film (NiFe-31) of approximately 600nm thickness was grown on a silicon substrate. Using the VSM, a hysteresis curve was generated for the film. The unetched film had a coercivity of 1.33 Oe and a magnetic moment of 6.43×10^{-2} emu. The curve was also unskewed. The film was then dipped into a diluted Al etch for thirty seconds, cleaned with water, and then blow dried.

A hysteresis curve for the 30-sec etched film yielded a coercivity of 1.42 Oe and a magnetic moment of 6.16×10^{-2} emu. The hysteresis curve also showed a definite skew to it. When the film was dipped into the etchant for another 30 seconds, the film detached from the substrate. Apparently, there was a large stress between the film and the substrate, and the acid etch ate away at the connection between the two.

The increase in coercivity, as well as the skewing, from the unetched film to the 30-sec etched film was probably caused by the relaxation of the film as it was becoming detached from the substrate

550nm NiFe 35%

The same procedure as above was performed on a nickel-iron film (NiFe-35) of approximately 550nm thickness. Again, as above, the film

detached during the second 30-sec etch, although signs of detachment were visible after the first 30-sec etch (the film appeared ruffled in places). The unetched film had a coercivity of 0.45 Oe and a magnetic moment of 0.29 emu. The 30-sec etched film had a coercivity of 0.52 Oe and a magnetic moment of 0.26 emu. The hysteresis curve did not skew between the unetched film and the 30-sec etched film, but there was an increase in coercivity. However, the tails of the 30-sec etch film did not come together as quickly as they did for the unetched film. The increase in coercivity and the thickening of the tails are both probably due to the relaxation of the film as it detached from the substrate.

5.2 Estimated Deposition Rate

To estimate the film thickness and deposition rate, samples of NiFe 35% and NiFe 45% on silicon were measured in an LDJ 9500 Vibrating Sample Magnetometer. The VSM was initially calibrated with a Nickel sample. Also, all measurements were made with the magnetic field applied parallel to the film surface. 1024 sample points were taken to form a complete hysteresis loop, and the peak field was set to 50 gauss.

The measured magnetic moment was used to estimate the film thickness. First, the saturation magnetization was determined from literature¹⁴.

$$M_s (\text{NiFe-35\%}) = 1053 \text{ emu}\cdot\text{cm}^{-3}$$

Then the surface area was computed for each sample.

The surface of a 1" diameter wafer is $\pi \cdot (1.27\text{cm})^2 = 5.067 \text{ cm}^2$.

NiFe-35% would give a signal of $1053\text{emu}\cdot\text{cm}^{-3} \cdot 5.067 \text{ cm}^2 \cdot 100\text{cm/m}$ or approximately $5.335 \cdot 10^5 \text{ emu/m}$.

For sample 102601-03 (NiFe-35%), the magnetization is $2.75 \times 10^{-2} \text{ emu}$. The thickness is then

$$2.75 \times 10^{-2} \text{ emu} / 5.335 \cdot 10^5 \text{ emu/m} = 51.5 \text{ nm}.$$

Table 5-2 shows the calculations for all samples measured.

Sample id	Sputter time	Composition	M [emu]	Hc [Oe]	Estimated thickness
On Silicon					
102601-03	2.36	NiFe-35%	$2.75 \cdot 10^{-2}$	2.94	51.54 nm
102601-02	3.56	NiFe-35%	$3.98 \cdot 10^{-2}$	1.95	74.59 nm
102601-04	5.55	NiFe-35%	$5.797 \cdot 10^{-2}$	2.90	108.6 nm
102501-03	8.35	NiFe-35%	$9.025 \cdot 10^{-2}$	1.621	169.1 nm
102501-01	13.20	NiFe-35%	$13.14 \cdot 10^{-2}$	1.22	246.3 nm
102501-04	20.00	NiFe-35%	$21.95 \cdot 10^{-2}$	0.7095	411.4 nm
102501-02	30.00	NiFe-35%	$29.26 \cdot 10^{-2}$	0.545	548.4 nm
102601-01	46.24	NiFe-35%	$45.76 \cdot 10^{-2}$	0.488	857.6 nm
On Silicon					
102801-04	2.36	NiFe-45%	$2.39 \cdot 10^{-2}$	15.14	39.42 nm
102801-01	3.56	NiFe-45%	$3.67 \cdot 10^{-2}$	22.65	60.53 nm
102801-02	5.55	NiFe-45%	$5.684 \cdot 10^{-2}$	13.95	93.76 nm
102701-01	16.30	NiFe-45%	$17.48 \cdot 10^{-2}$	2.26	288.3 nm
102701-04	21.00	NiFe-45%	$24.10 \cdot 10^{-2}$	1.26	397.5 nm
102701-03	31.00	NiFe-45%	$35.01 \cdot 10^{-2}$	1.32	577.5 nm
102701-02	46.00	NiFe-45%	$48.74 \cdot 10^{-2}$	4.14	803.4 nm
	72.00	NiFe-45%	Pealed off substrate lost		
Samples on Glass					
102401-04	3.45	NiFe-35%	$2.91 \cdot 10^{-2}$	4.39	72.7 nm
102401-03	7.30	NiFe-35%	$5.30 \cdot 10^{-2}$	2.7	132.4 nm
102401-02	15.00	NiFe-35%	$11.03 \cdot 10^{-2}$	1.44	275.6 nm
102401-01	30.00	NiFe-35%	$21.14 \cdot 10^{-2}$	0.628	528.1 nm

Table 5-2 Estimated thickness from VSM measurements

The measured magnetization can be used to estimate the film thickness, and to calculate the deposition rate. The estimated thickness of the first eight samples in Table 5-2 was plotted against their sputter time. The result is shown in Figure 5-3.

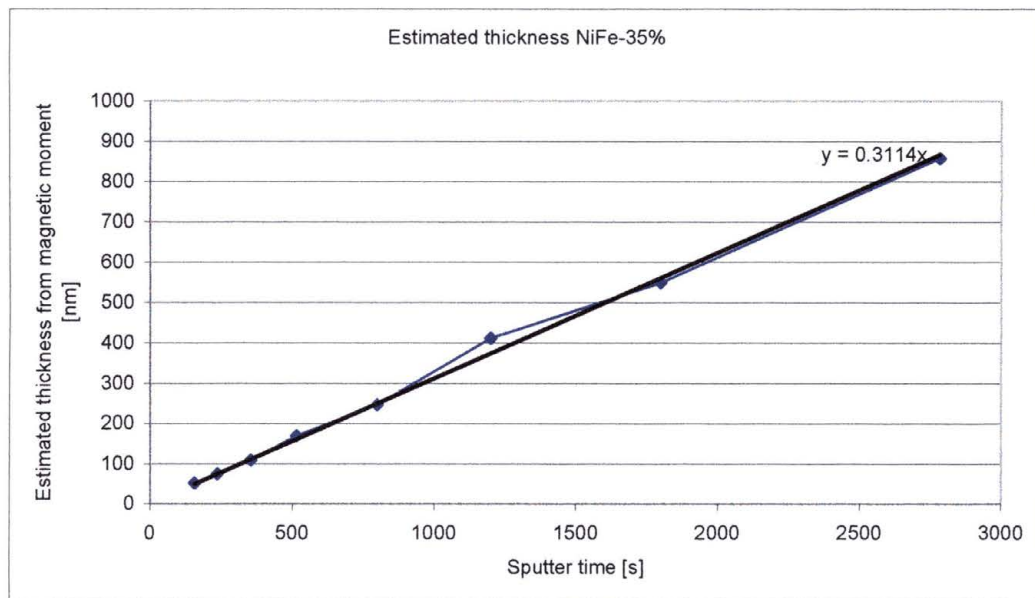


Figure 5-3 Sputtering time vs. estimated thickness

The calculated deposition rates for all three groups were:

NiFe-35%: 3.144 A/s

NiFe-45%: 2.983 A/s

NiFe-35%: 2.962 A/s

These are the estimated linear sputter rates. In practice, sputter rates tend to increase as a function of time.

The sputter rate of the NiFe-45% should be typically a little lower than the sputter rate for the NiFe-35% target as the former target is more magnetic. The magnetic flux and density of the plasma is thus less above the NiFe-45% target. The differences observed here are marginal.

5.3 Hysteresis of an Unattached Thin Film

In order to determine the effects of stress on an as-sputtered film, the hysteresis loop of a NiFe-45% sample was measured from a film as-sputtered, and after the film detached from the substrate.

The hysteresis loop of an as-sputtered film is shown in figure 5-4.

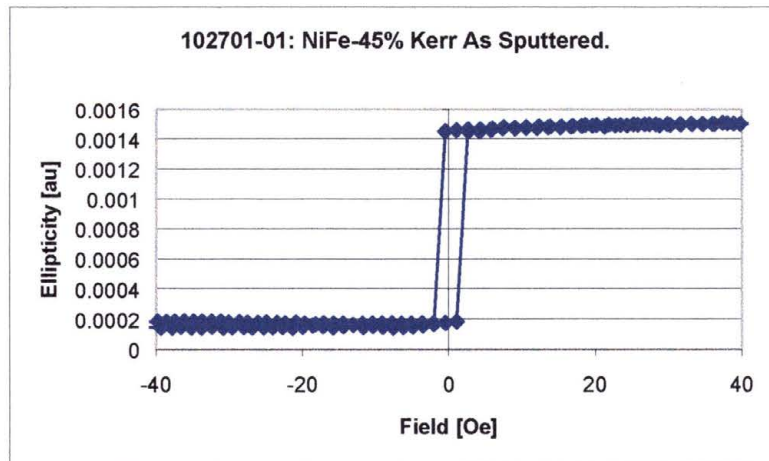


Figure 5-4 Hysteresis loop of a NiFe 45% thin film as-sputtered

During ultrasonic cleaning, the film spontaneously peeled off of the substrate. The hysteresis loops were again measured from the sample. One loop was taken from each side of the unattached film. Figure 5-5 shows the hysteresis loops for both sides of the thin film.

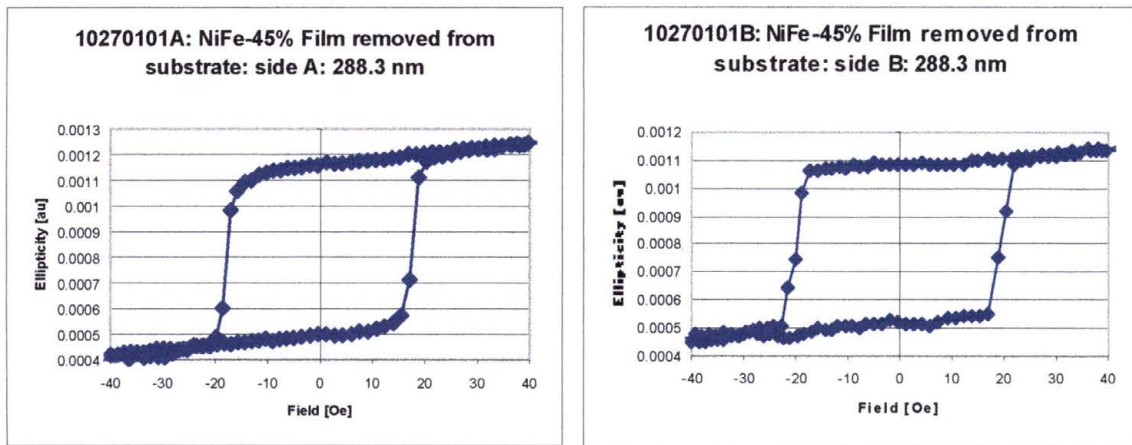


Figure 5-5 Hysteresis loops of both sides of the unattached thin film

The measured coercivities are:

H_c (VSM) as sputtered: 2.24 Oe

H_c (Kerr) as sputtered: 1.85 Oe

H_c (VSM) removed from substrate: 15.33 Oe

H_c (Kerr) removed from substrate: 17.7 Oe

Results between the Kerr and VSM measurements are similar in each case. The differences between the Kerr and VSM measurements may be due to the instruments not being in relative calibration.

Also, the VSM measurements of the unattached sample may be in error due to the condition of the thin film. When the unattached sample

was measured, it contained folds, and was no longer everywhere flat with the substrate.

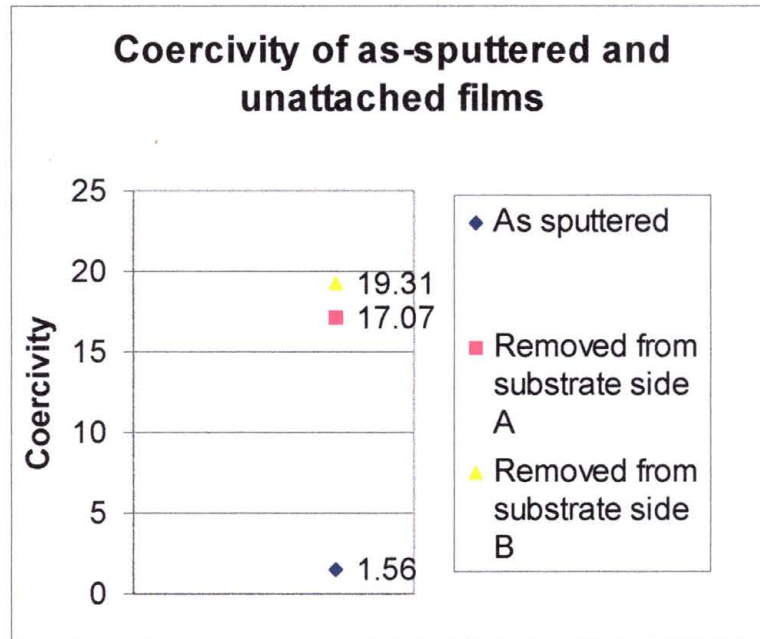


Figure 5-6 Magnitudes of the coercivity of as-sputtered and unattached thin films

There is a drastic change in coercivity between the as-sputtered film and the unattached film. We believe this is due to the stress that the as-sputtered film is under. This will be examined further in the next chapter.

5.4 Hysteresis Loops of Various Film Thicknesses

Appendix A shows hysteresis loops for 8 samples of increasing thickness. The Kerr hysteresis loops are in the left column, and the VSM loops are in the right column.

The hystereses measured by VSM are much more rounded than those measured by the Kerr tracer. Particularly the thinnest film, which shows a very straight approach to saturation in the Kerr curves.

As the film thickness increases the VSM curves become similar to the Kerr curves. The Kerr measurements use reflected laser light, and only penetrates 15-30 nm into the surface of the thin film. The focused spot size of the laser is .5 mm, so the Kerr measurements are local. The VSM measures the bulk properties of the material. Where the graphs show different hysteresis loops, the local surface magnetic properties can be considered to be different from the bulk properties of the thin film.

5.5 Scanning Kerr Measurements

To further investigate the local properties of the thin films with Kerr measurements, the optical Kerr effect was measured for small spot sizes across a sample. The sample was secured to a step-motor to

control the position in the y-axis. Measurements were made across the surface of the sample at every .5 mm.

These results were compared with Kerr measurements done using a very large spot size that covered the entire sample. Flood results from a glass substrate, seed layer (through the substrate) are shown in figure 5-7 for sample 10240104.

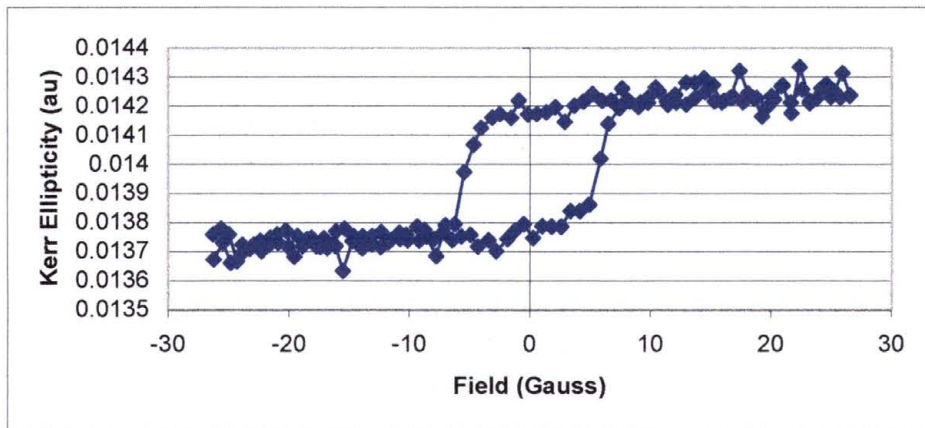


Figure 5-7 Kerr measurement for entire sample of NiFe on glass

This can be compared to a single point measurement with a laser spot size of .5 mm, shown in figure 5-8 for sample 10240104.

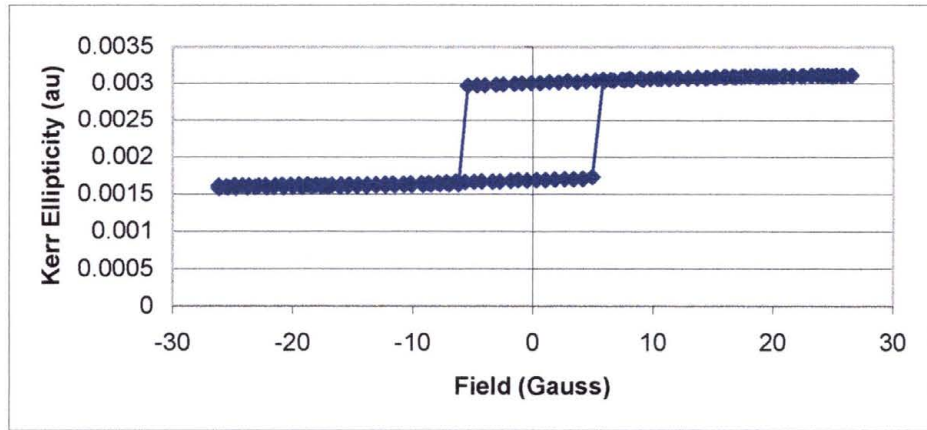


Figure 5-8 Kerr measurement with spot size of .5 mm

This sample produced a hysteresis curve which retained the same characteristics over the surface of the sample. Figure 5-9 shows a Kerr hysteresis loop at the bottom edge of the sample, and figure 5-10 shows a measurement at the center of the sample. The magnetization appears to be lower in amplitude and higher in noise at the center of the sample. This is because the laser was not centered on the photo-detector after the step motor moved the sample. The intensity of the laser was diminished.

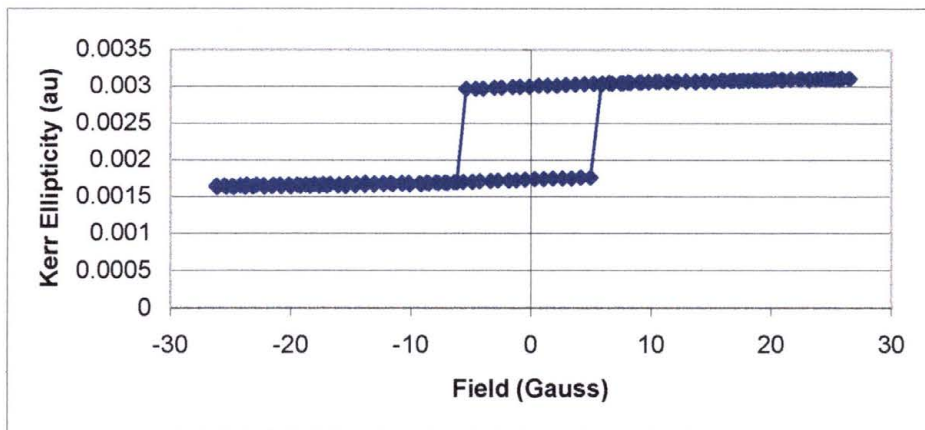


Figure 5-9 Hysteresis curve of a Kerr measurement at the bottom edge of sample 10240104

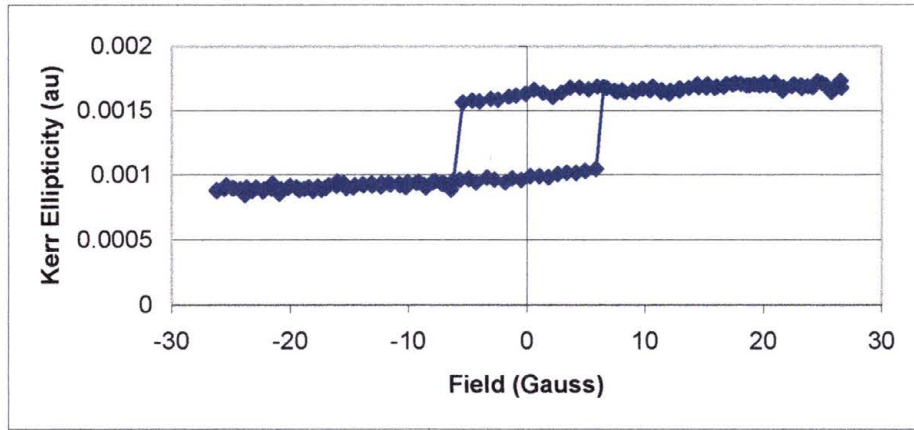


Figure 5-10 Kerr hysteresis loop at the center of sample 10240104

Sample 10260101 was also scanned, with less consistent hysteresis loops. Figures 5-11 through 5-13 show the variation in the hysteresis loops from the top, center and bottom of the sample. This could be due to the variation in stress or film thickness across the sample.

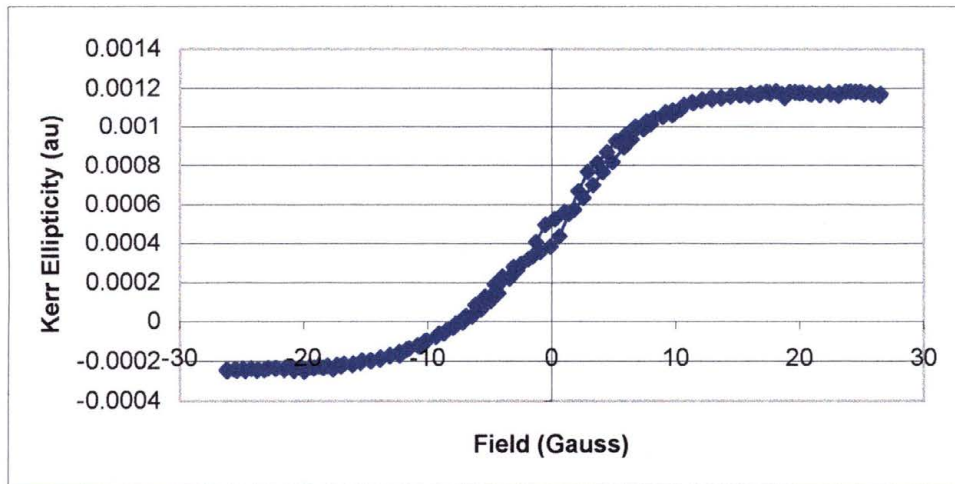


Figure 5-11 Hysteresis loop of the bottom edge of sample 10260101

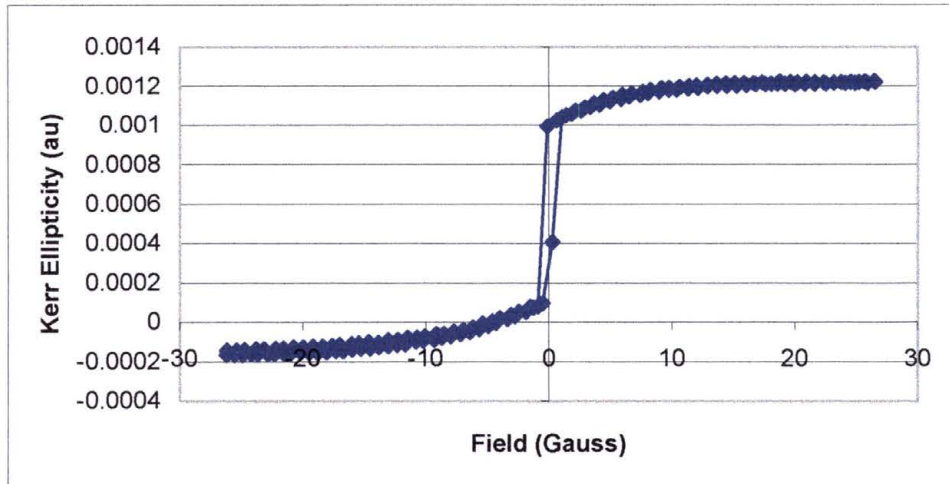


Figure 5-12 Hysteresis loop of the center of sample 10260101

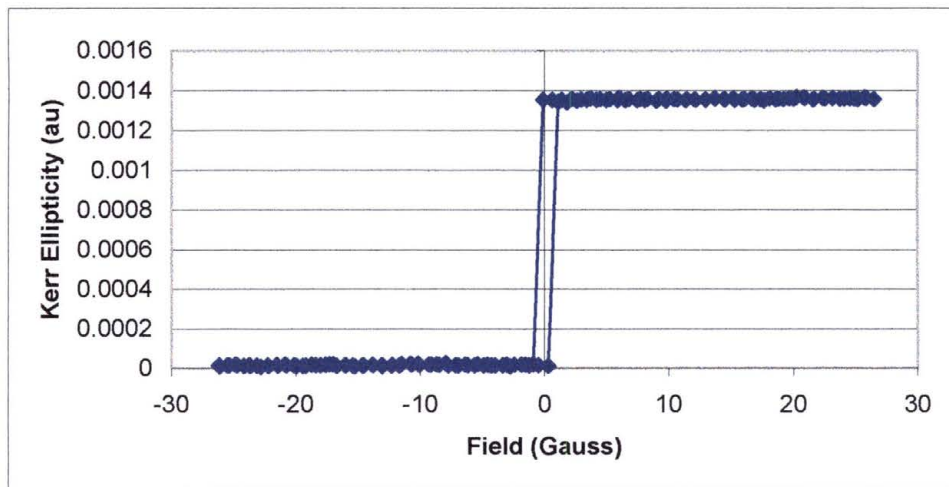


Figure 5-13 Hysteresis loop at the top edge of sample 10260101

A local variation was observed in sample 10260101 at a position 3 mm above the bottom edge of the sample. Figures 5-14 through 5-17 show the Kerr hysteresis loops of points .5 mm apart. This effect could

be due to magnetic domains. More detailed scans would have to be performed to confirm this.

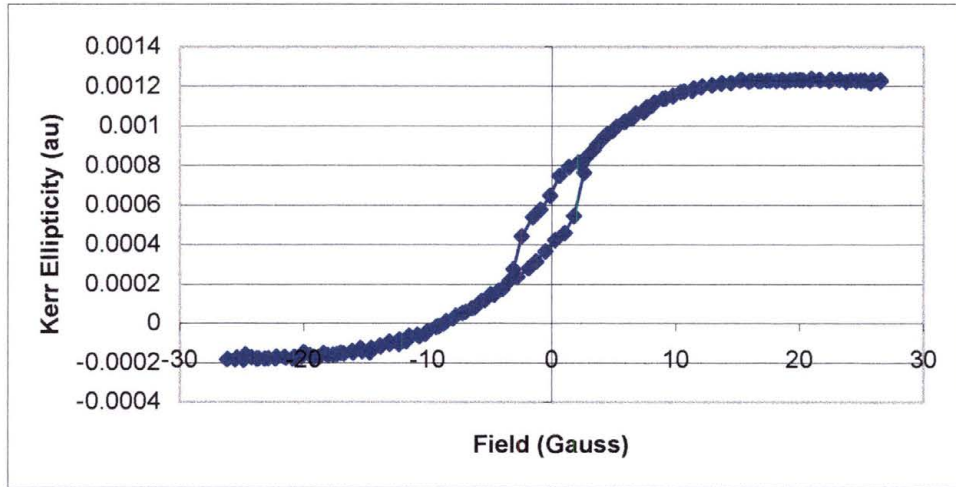


Figure 5-14 Kerr measurement at 3 mm from bottom edge of sample 10260101

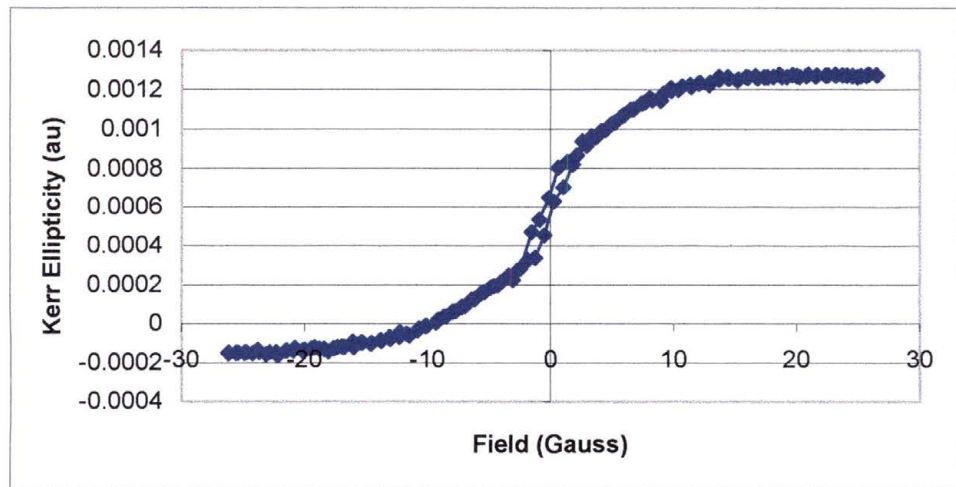


Figure 5-15 Kerr measurement at 3.5 mm from bottom edge of sample 10260101

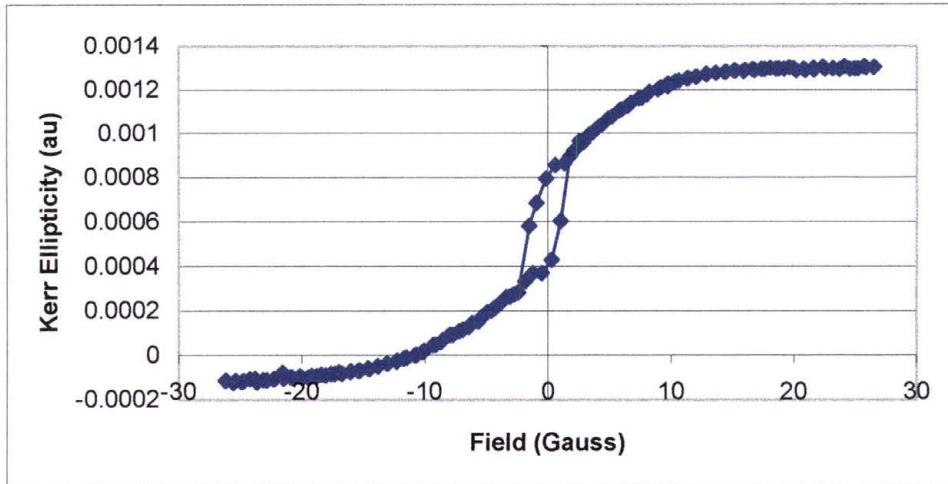


Figure 5-16 Kerr measurement at 4 mm from bottom edge of sample 10260101

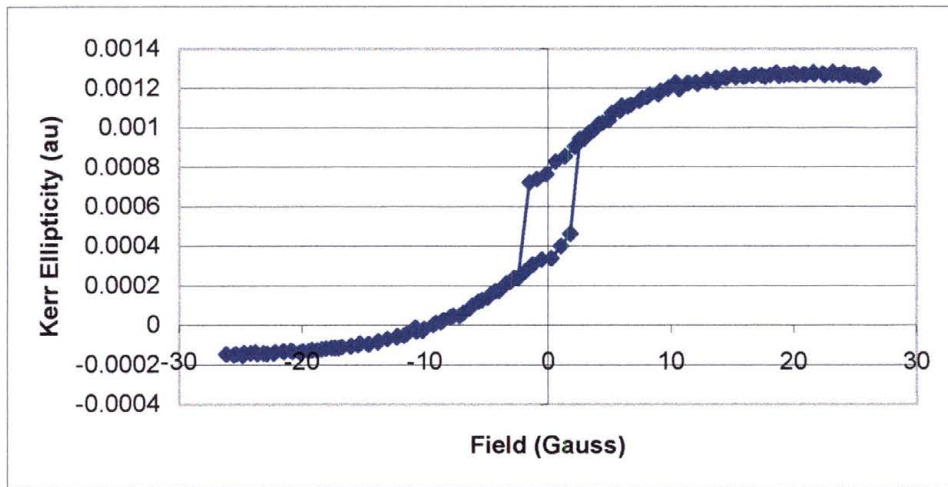


Figure 5-17 Kerr measurement at 4.5 mm from bottom edge of sample 10260101

5.6 Coercivity vs. Film Thickness

The hysteresis curves NiFe 35% films on glass were measured. The coercivity is observed to decrease with increasing film thickness. Figure 5-18 shows that as the film thickness ranges from 72 to 528 nm, the coercivity ranges from 4.53 to 0.65 Oe.

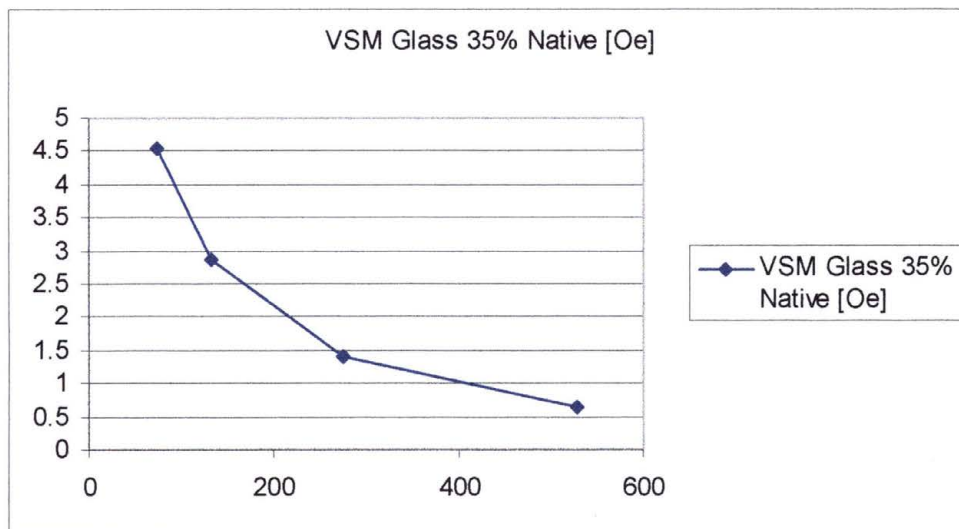


Figure 5-18 Coercivity vs. film thickness

Figure 5-19 shows the same relation for films sputtered on silicon (NiFe 45%). The same decreasing coercivity is seen. However, at the smallest thickness of film measured (39.42 nm), the coercivity is seen to drop.

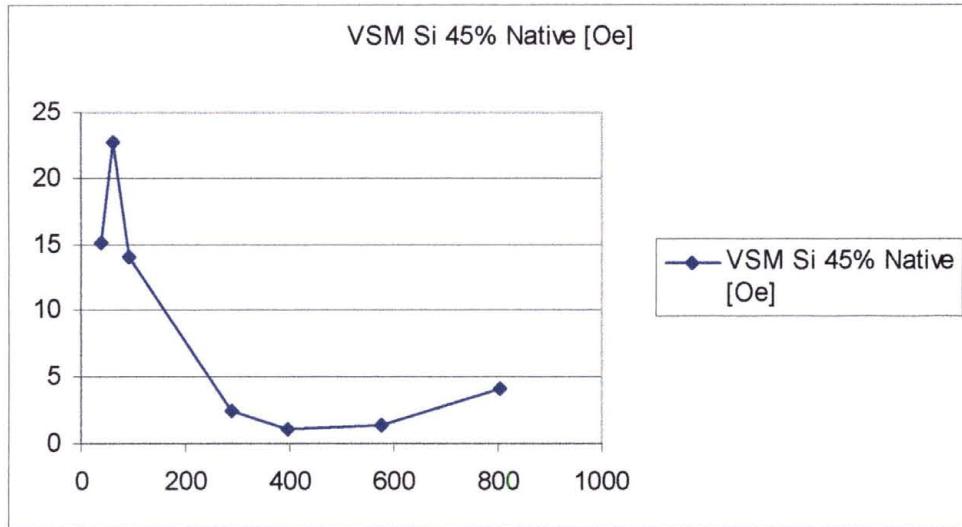


Figure 5-19 Coercivity vs. film thickness for NiFe 45%

Figure 5-20 shows hysteresis curves measured both by VSM and Kerr. As the thickness of the films decreases, the coercivity increases down to a film thickness of just below 200 nm. Both data sets drop in coercivity, and then rise again. Only the Kerr data set shows the coercivity dropping again at the thinnest film thickness.

Some of this could be explained by measurement error. However, the thicker film series looks consistent.

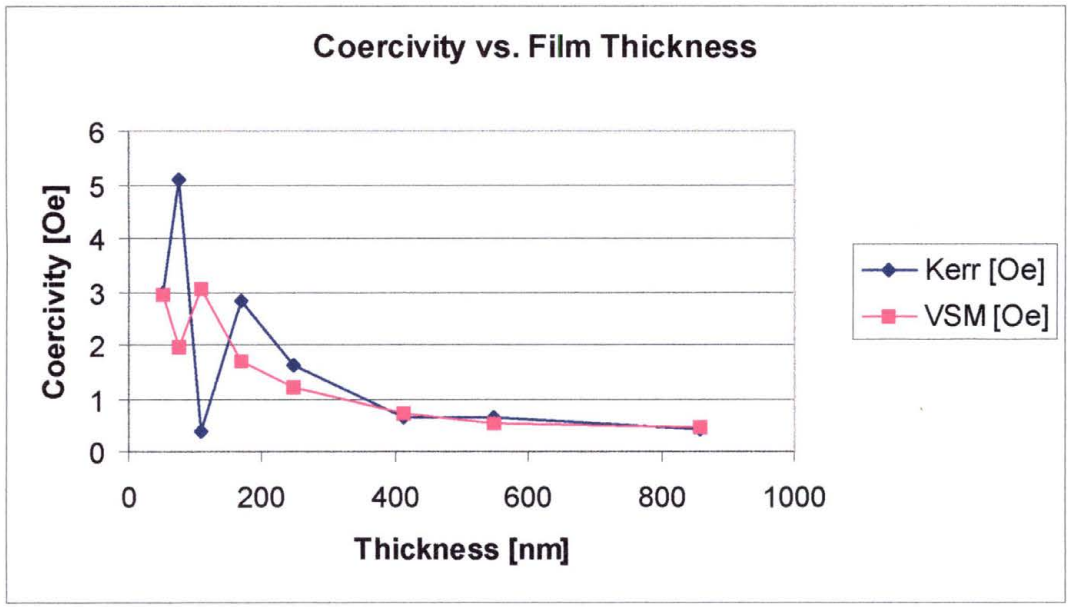


Figure 5-20 Coercivity vs. thickness measured by VSM and Kerr

To take a better look at the coercivity vs. thickness, we can examine the series of thin films that was used to measure the etch rate (see appendix A). The magnetization can be used to estimate the film thickness. The coercivity was plotted vs. magnetization to examine how the coercivity varies with film thickness (Figure 5-21).

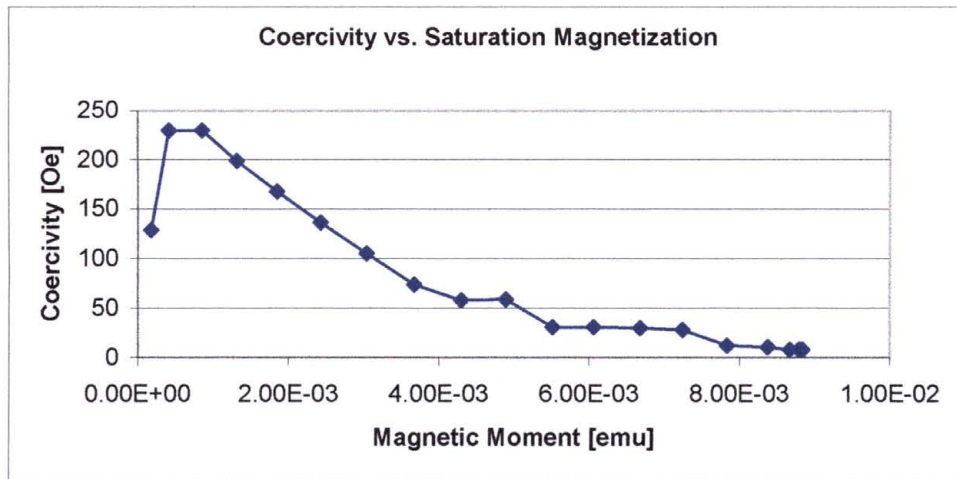


Figure 5-21 Coercivity vs. saturation magnetization

The final decrease of coercivity is seen in the measurements of the thinnest films. The point at which this occurs can vary. This may be due to the properties of the films, or the stress.

CHAPTER 6

PATTERNED THIN FILM MEASUREMENTS

6.1 Stress Observed by the Stylus Profilometer

Samples were measured with a Tencor 500 Profilometer. This instrument uses a stylus with a 5 micron diameter to scan across a sample with 10 milligrams of force. A height profile of the scan is recorded.

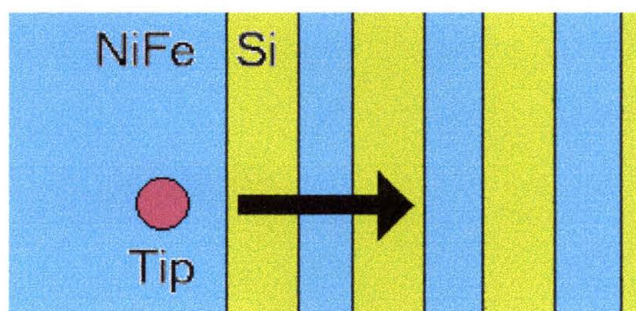


Figure 6-1 Scan of a Patterned Thin Film

Figure 6-1 shows the direction of the scan across a grating pattern. The scan is initiated on the unpatterned thin film, and moves onto the patterned area, perpendicular to the etched parallel lines that define the grating.

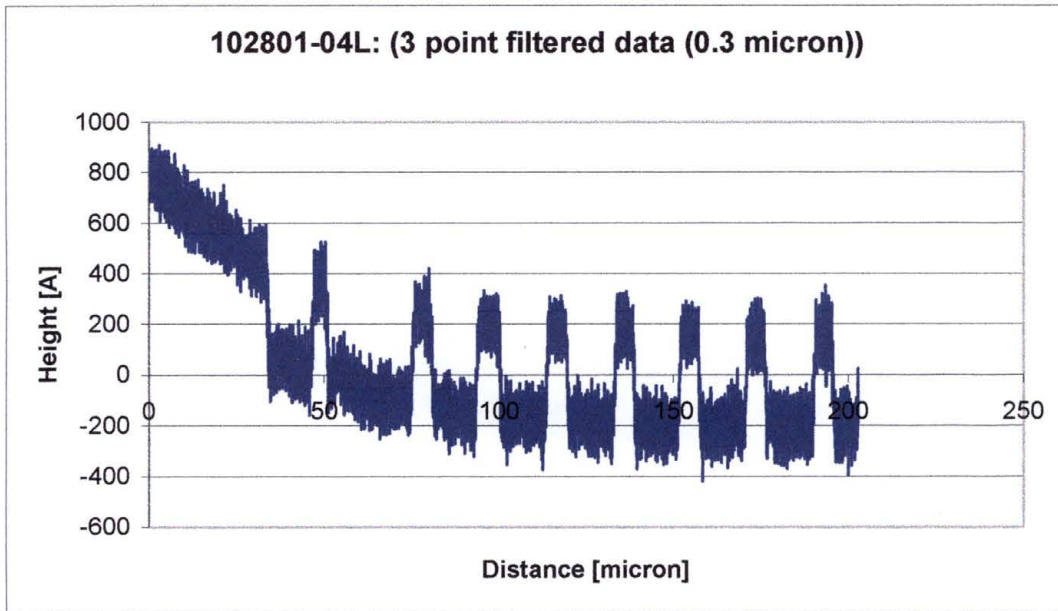


Figure 6-2 Scan of Sample 102801-04

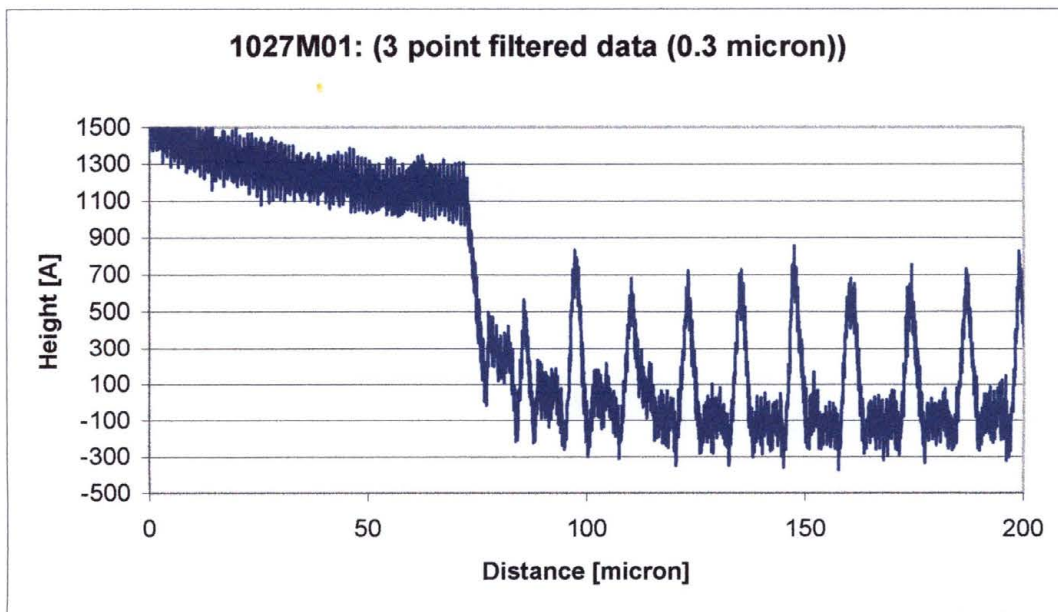


Figure 6-3 Scan of Sample 102701

Figures 6-2 and 6-3 show the scans of two samples starting at the edge of the patterned area. The unpatterned area (on the left) shows a

curvature. This is due to the stress of the unpatterned thin film. The patterned area appears to be flat. This may be due to the fact that the stress has been relieved by the patterning of the thin film, perpendicular to the grating.

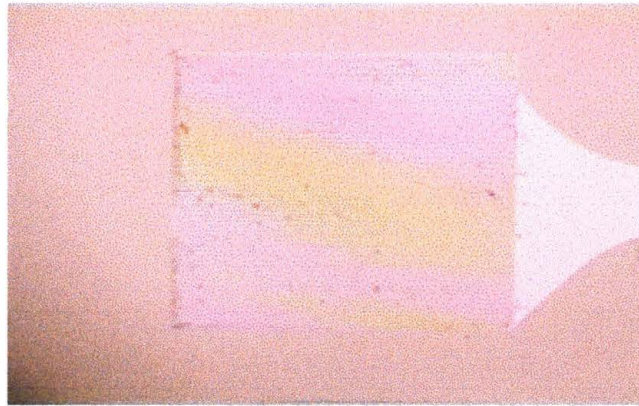


Figure 6-4 Patterned Area where Thin Film Spontaneously Peeled Away

The effect of stress on unpatterned areas has been examined in practice. Figure 6-4 shows a thin film, which during etching, peeled off of the entire sample except for the patterned area and a small area to the right of the thin film.

6.2 Pattern Sizes Measured By Stylus Profilometer

The profile of the patterns can be observed from the Profilometer data as well. Figures 6-5 through 6-7 show profiles from the sample 102501. This sample has a film thickness of 223 nm.

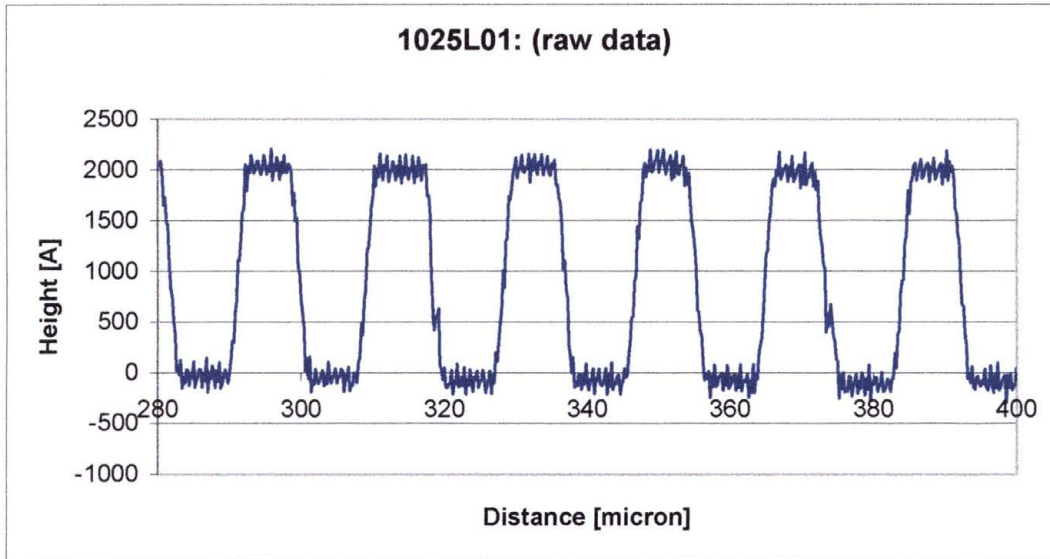


Figure 6-5 Profile of 5 micron wide lines

Figure 6-5 shows that the profiles of the lines are flat on top. The height of the lines is also the thickness of the unpatterned film. The etching was complete (down to the silicon). The sides of the lines are not exactly vertical, but this could be due to the diameter of the radial stylus (5 microns).

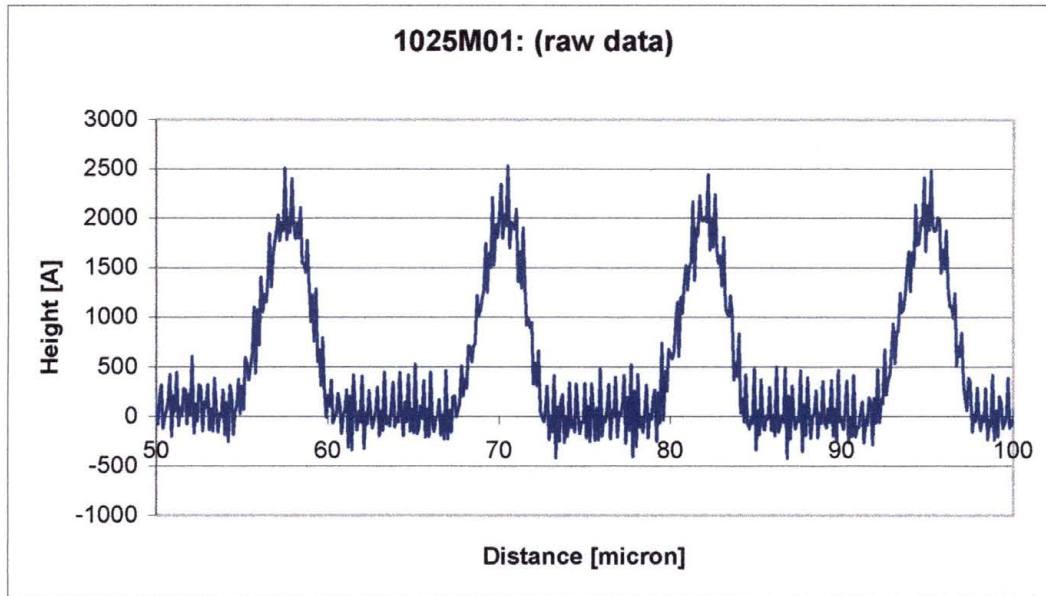


Figure 6-6 Profile of 1.55 micron wide lines

Figure 6-6 shows the profile of the pattern with 1.55 micron wide lines. The tops of the lines reach the full thickness of the thin film, but they are not flat. This is due in part to the stylus, and in part to the etchant. For the thinner lines, the photoresist loses adhesion. This has been observed by microscopic examination (the photoresist lines appear to warp). The etchant starts to dissolve the metal under the photoresist starting at the edges.

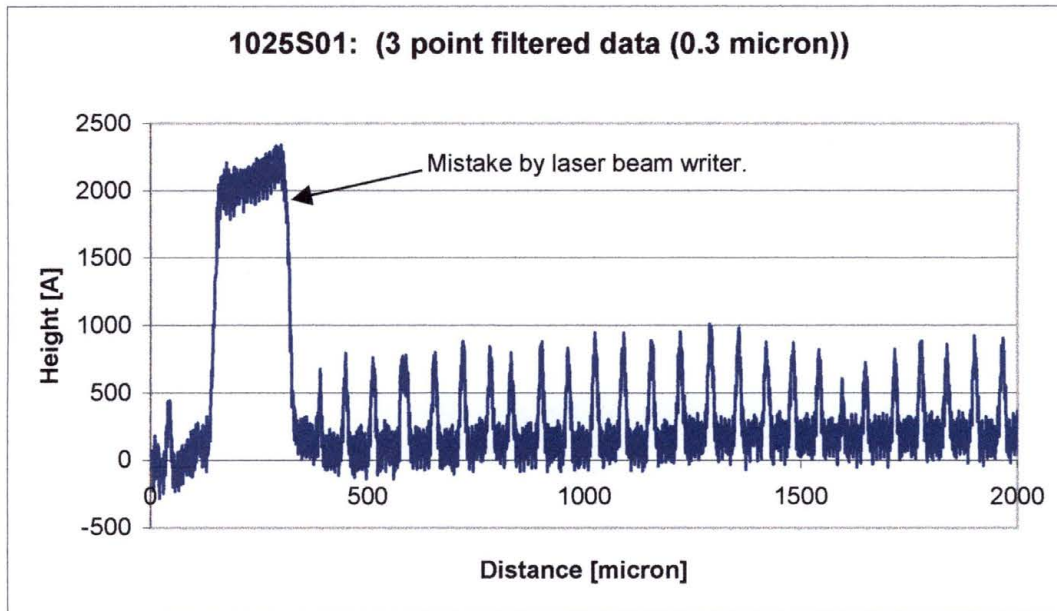


Figure 6-7 Profile of 0.9 micron wide lines

Figure 6-7 shows the profile of 0.9 micron lines. The lines are clearly not as high as the original thin film. This is observed by the area where the laser writer mistakenly skipped over 250 microns. The tops of the lines are also not flat. For the thinnest lines, the photoresist was completely dissolved, and the lines were etched for too long.

Table 6-8 shows a summary of the profile measurements for other samples.

Sample	Period ³	Line Width ¹	Line Height ²	Film Thickness	Rise Time ⁴	Line Width at base
102501-01 L	18.26 μm	5 +/-0.5 μm	223 nm	223 nm	3 μm	
102501-01M	12.54 μm	1.55+/- .5 μm	207 nm	223 nm	2.4 μm	
102501-01S	6.3 μm	0.9+/- .2 μm	56 nm	223 nm		
102701-01L	18.6 μm		100 nm	266 nm	3.5 μm	7 μm
102701-01M	12.62 μm		71 nm	266 nm	2.55 μm	5.1 μm
102701-01S	6.1 μm		18 nm	266 nm		1.5-1.8 μm
102601-02M	12.7 μm	3.9+/.1 μm	64 nm	64 nm	1 μm	
102601-02S	6.2 μm	2.5+/- .2 μm	10 nm	64 nm		
102801-04L	19 μm	5.2+/-0.4 μm	36 nm	36 nm	1-1.3 μm	
102801-04M	12.5 μm	0.5-1 μm	36 nm	36 nm		3 μm
102801-04S						

- 1) Width of the line where the height is 95% of the maximum; Range caused by variation of the line width. Range determined by measuring two arbitrary line widths.
- 2) Corrected for by re-calibration.
- 3) Averaged over at least 4 periods.
- 4) Measured rise time on discrete step of film 102501-01: 1.4 μm .

Table 6-8 Profilometer Results of Patterned Thin Films

6.3 Hysteresis Curves of Patterned Thin Films

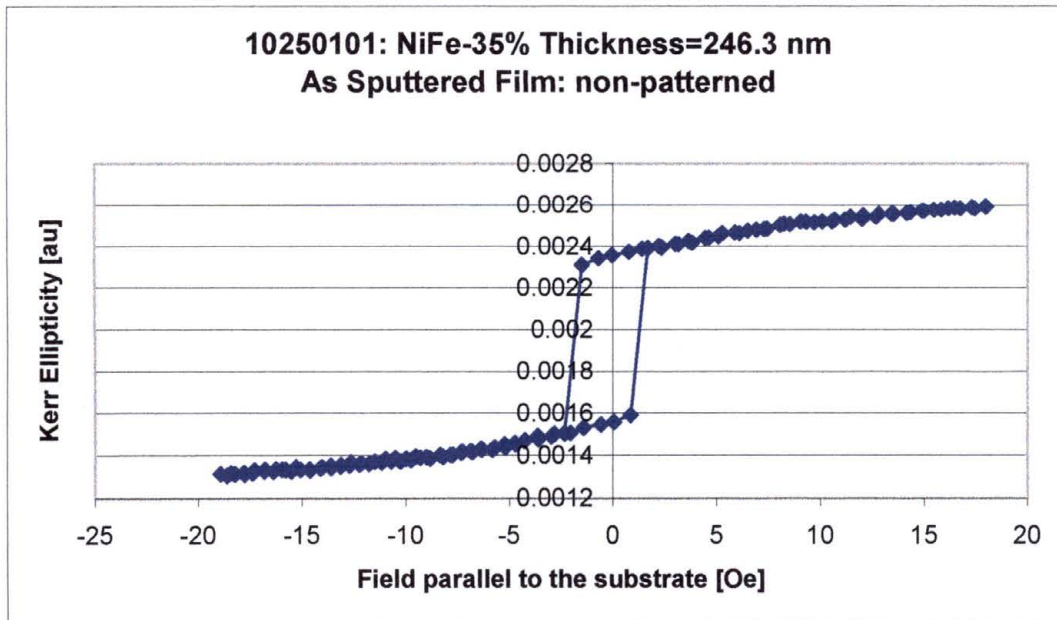


Figure 6-9 Sample 10250101, Unpatterned Area of Thin Film

Figure 6-9 is a Hysteresis curve of sample 10250101 from an unpatterned area. Figure 6-10 shows six hysteresis curves from the same sample. All of the hysteresis curves in figure 6-10 were taken from patterned areas.

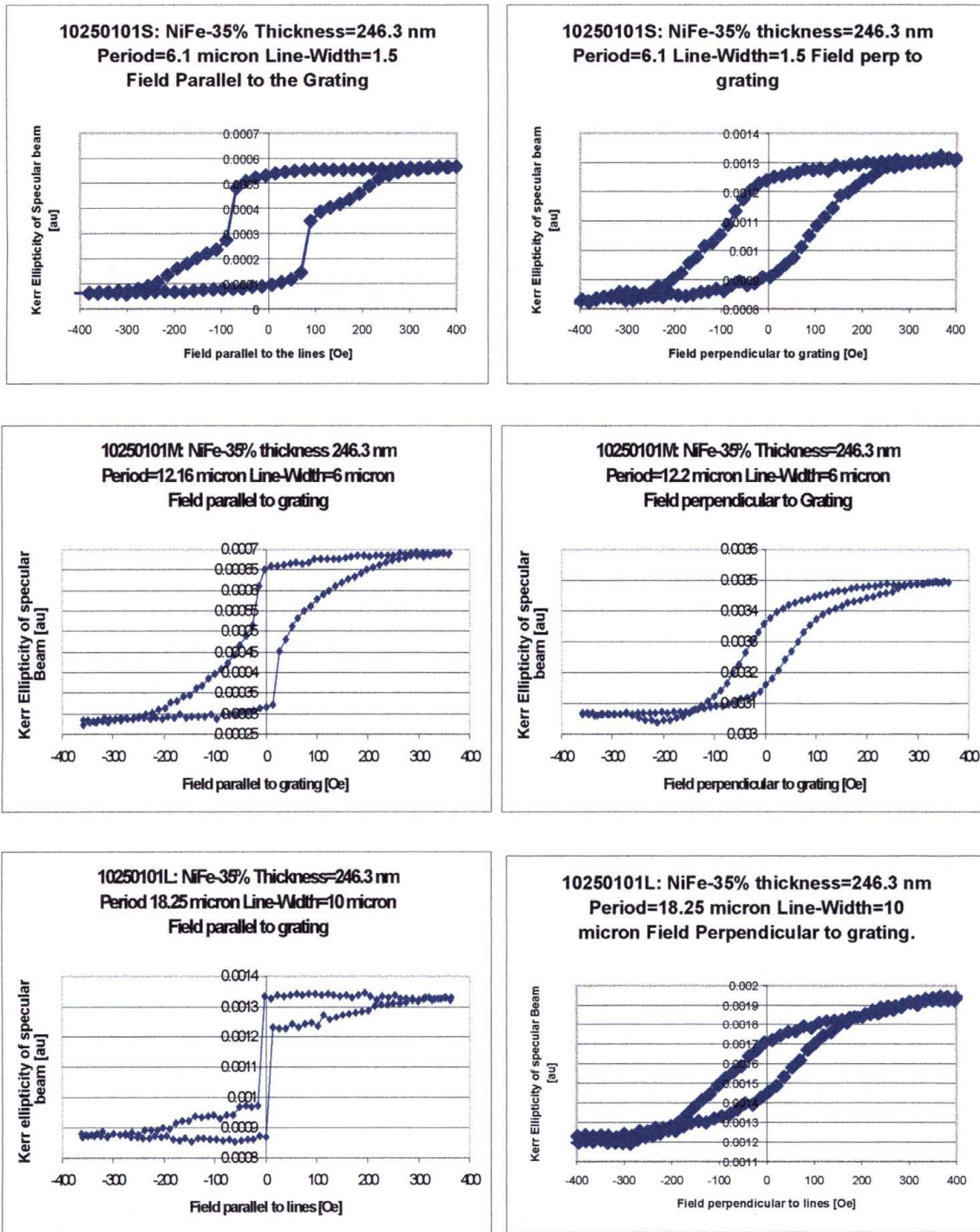


Figure 6-10 Six Hysteresis curves from the Patterned Area of Sample 10250101

The curves on the left of Figure 6-10 were taken with the applied magnetic field parallel to the grating. The curves on the right were taken with the applied field perpendicular to the grating.

The Hysteresis curves of figure 6-10 are also ordered by the line sizes in the gratings. The top two curves were measured on the grating with a line width of 1.5 microns, and a period of 6.1 microns. The middle two curves have a line width of 6 microns, and a period of 12.16 microns. The bottom two curves have a line width of 10 microns, and a period of 18.25 microns.

The Hysteresis curve of sample 10250101 (Figure 6-9) shows a coercivity of 2-3 Oe. This is less than any of the hysteresis curves of Figure 6-10 from the patterned areas of the same sample.

6.4 Strain

At least one factor in the coercivity is the strain on the thin film in the patterned areas vs. the unpatterned areas. The profilometer data in Figures 6-2 and 6-3 show that the samples are curved in the unpatterned area due to stress, and that the stress is less in the patterned areas.

Figure 6-10 also shows a difference in the coercivity between the graphs on the left and the graphs on the right. The coercivity is the same or less for the hysteresis loops on the left (with the field parallel to the gratings). This is more obvious in the bottom two figures (with the

largest line width). The stress in this case is tension along the parallel lines, pulling parallel to the grating lines. Perpendicular to the lines, there is not as great of a pulling force, because the material has been etched away.

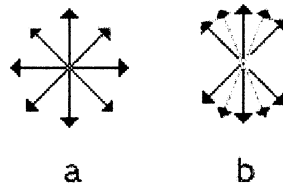


Figure 6-11 a) Isotropic distribution of domain orientations b) Effect of tension in the vertical direction¹

NiFe 35% has a positive magnetostriction value. Figure 6-11 shows the effect of tension on the distribution of domains. Tension lines up more domains, and makes it easier to magnetize along the same axis as the applied tension. Therefore, the coercivity is lower parallel to the applied tensile stress.

6.5 Demagnetizing Factor

The strength of the internal field depends on the external field, and a demagnetizing factor.

$$H_{int}=H_{ext}-H_d$$

This equation also shows how the demagnetizing field, H_d , opposes the external field H_{ext} , and the internal field H_{int} .

A magnetic material responds to an applied magnetic field by creating North and South poles of its own. These poles create an opposing field called a demagnetizing field.

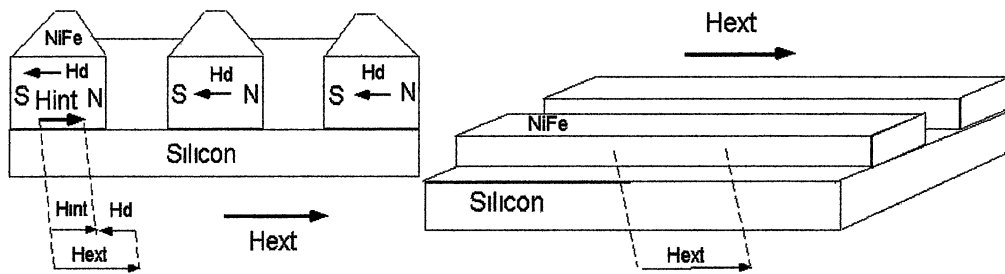


Figure 6-12 (a) Externally Applied Field Perpendicular to the grating; (b) Externally Applied Field Parallel to the grating. In the latter case there are no free poles and thus no demagnetizing field.

Figure 6-12 shows the orientation of grating lines with respect to their demagnetizing field, and the applied field. When a thin film grating is magnetized perpendicular to the grating lines, the demagnetizing field is greater than if it is magnetized parallel to the lines. This is because there are more field lines permeating the sample, per unit volume.

The demagnetizing factor is a ratio of the sample geometry. If a sample can be considered to be infinitely long and magnetized parallel, the demagnetizing factor will be zero.

If the demagnetizing field is less, the sample will be easier to magnetize, and the coercivity will be lower in this direction. Since the demagnetizing field is less parallel to the grating lines, and greater perpendicular to the grating lines, the coercivity should be less parallel and greater perpendicular to the grating lines.

The demagnetizing field can also be expressed as the product of the demagnetizing factor and the magnetization. There is one demagnetizing factor for each dimension of the sample (N_x , N_y , N_z). For example, in the x direction $H_d=N_x*M$.

6.6 Domain Size

As the line width and thickness approaches the domain size of NiFe 35%, the hysteresis will change drastically. Single domains of nickel-iron as large as 8 mm have been observed to exist in thin films¹⁴.

A scanning laser microscope can measure domain sizes with a resolution of 10-100 microns. A Bitter colloid may have adequate results to show the domain sizes. These techniques can be used to measure domains in as-sputtered and patterned films and compared. The domains in different sized gratings can be compared also.

Although we have not studied the domain patterns in our films, the large differences between the VSM and Kerr curves (as reported in chapters 5 and 6) suggest that domain size is larger than the created structures.

6.7 Homogeneity of the Film Thickness over the Sample Surface

Grating patterns were etched onto 1" silicon wafers. During the etching process, part of the thin film detached from the silicon for two of the samples, 102501-01 and 102701-01. This created a perfect, discrete step between the surface of the silicon and the thin film.

These two samples were examined to determine the uniformity of the surface film thickness over the 1" wafer. Scans with the stylus profilometer were made from an area without film to an area with film.

For sample 102501-01 (NiFe-31%), film thickness was measured near the center and near one edge:

center: 218 nm

edge: 216 nm

From this we may conclude that the variation of the thickness over the film surface is less than +/- 0.5 %.

For sample 102701-01, film thickness was measured on 10 different locations on the 1 inch wafer. See figure 6-14 for the locations

and the results. From these results we may conclude that the variation of the thickness over the film is less than +/- 5%. The larger thickness variation for this film might be due to the fact that the target does not have the same thickness everywhere. In order to be able to light this target, we had to turn it down on the lathe to make it thinner.

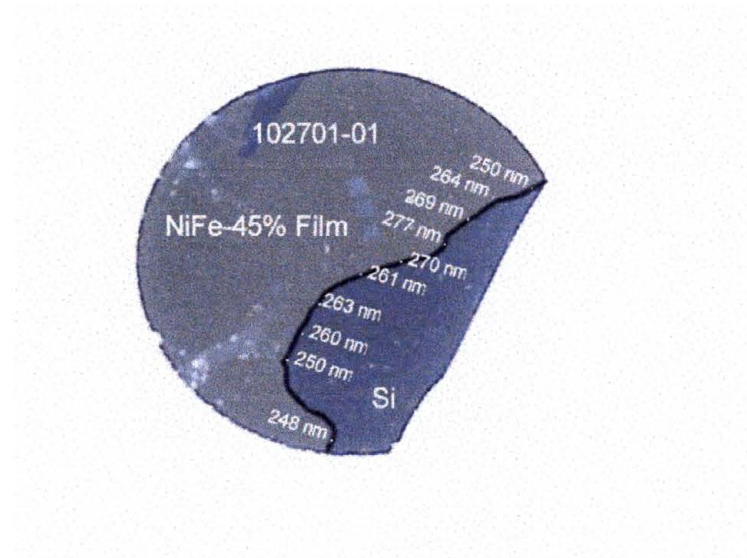


Figure 6-13 Film thickness measurements over a 1" silicon wafer

We conclude from these measurements that the film thickness is almost constant over the film.

CHAPTER 7

CONCLUSIONS

Sub-micron sized structures were manufactured with a laser writer.

An etch rate of 5.6 Angstroms per second was recorded for NiFe 35% using diluted Al etchant.

The coercivity of an unattached film was observed to be larger than an as-sputtered film.

Patterning thin films increases the coercivity. This is believed to be because the patterning relieves the stress.

Thinning of the film (by etching) will increase the coercivity.

The hysteresis of the patterned thin film depends on the orientation of the grating with respect to the magnetic field.

The worst case thin film homogeneity was +/- 5% over the surface of a 1" wafer.

CHAPTER 8

IDEAS FOR FURTHER RESEARCH

8.1 Measuring Magnetic Hysteresis during Etching

In order to investigate the wet etching process in more detail, the Kerr measurements can be taken in situ. Figure 8-1 shows an example configuration.

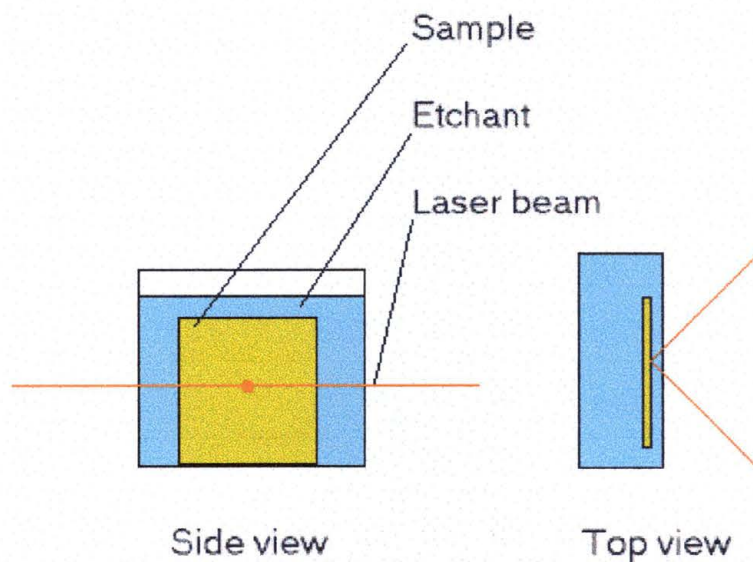


Figure 8-1 Configuration for Kerr measurements during etching

A sample is placed in a rectangular beaker that is filled with etchant. The etchant can be diluted further to slow the etch rate. Kerr measurements can be taken by selecting a spot on the sample with the laser and using the computer to collect data. The properties of the thin films could be compared to the VSM measurements for samples that were etched periodically.

Structured samples could also be measured. A sample with a grating pattern would show changing magnetization as the grating lines became thinner. This could help isolate the origin for the changes in the hysteresis curves for smaller structures.

8.2 Effects of Stress on Patterned Thin Films

The stress could be better understood if it could be isolated. If a sample were to undergo stress applied to it to relieve the tension either parallel or perpendicular to the grating, this may influence the hysteresis curve independent of domain size and demagnetizing factors.

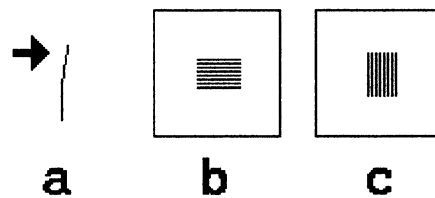


Figure 8-2

a) Side view of sample under applied stress b) Front view, perpendicular to grating c) Front view, parallel to grating

Figure 6-2 (a) shows the side view of a grating sample with pressure applied to the back of the sample. Figure 6-1 (b) and (c) show the front of the sample for perpendicular and parallel orientations of the pressure with respect to the grating. The pressure should relieve some of the tension in the etched lines of the grating. A change in the hysteresis curve would help explain the role of stress.

8.3 Temperature Sensitivity Measurements

Because of the temperature sensitivity of metallic thin films, a temperature of 1 °C can be about equal to the entire magnetostriction effect being measured¹⁴ (p250).

The thermal expansion coefficient for Silicon is $4.15 \times 10^{-6} / ^\circ\text{C}^{15}$, and for NiFe 36% is $0.7 \times 10^{-6} / ^\circ\text{C}^{16}$. Silicon therefore expands to a greater degree than NiFe when heated. The degree to which this affects the magnetization could be measured.

This could be done with a temperature sensor that relays data back to the controlling computer. The temperature of the sample then can be changed by heating the sample. A source of radiation could be a small lamp or heater, as long as the light does not interfere with the Kerr measurements.

As the sample is heated, hysteresis loops could be measured periodically and plotted. M_s and H_c could then be plotted with respect to time. It would be expected that as the sample was heated, the thin film would expand more than the silicon, and stress would be relieved on the thin film.

The reverse measurement could also be performed. The sample could be heated, and allowed to cool. Hysteresis loops could be measured as the sample cooled and compared to the loops that were measured as it was heated.

The loop closure should also change. When measurements are made during heating or cooling, the hysteresis loops should not close if there is a large enough temperature difference. The closure of the loops could be compared between heating and cooling. These heating effects could play an important role for patterned samples on glass.

8.4 Using the Laser Writer as a Profilometer

From Table 8-3, the depth of focus is 0.6 microns for the APO SL 100x lens. By autofocusing the alignment beam on the laser writer, the z coordinate position can be found to an accuracy of less than one micron.

	APO SL 50X	APO SL 100X
Numerical Aperture, NA	0.55	0.7
Working Distance, WD (mm)	13	6
Focal Length (mm)	4	2
Depth of Focus (microns)	0.9	0.6

Table 8-3 Specifications for the APO SL 50x and 100x lenses

By scanning a sample in a two dimensional grid, an autofocus command can be issued at regular intervals. The z coordinate (height) can be saved for each point on the grid.

From the saved data, a 3-dimensional representation of the sample can be reconstructed and analyzed for curvature. Curvature would be expected because of the observed stress of the thin films.

While scanning large grating patterns, it has been noticed that a systematic “drift” in the z axis takes place. For these gratings, an autofocus command is issued for every 5 minutes of scanning.

For profiling arrays that will take over 5 minutes to complete, a point should be designated to recalibrate the measurement, or to note any drift, so that the data can be renormalized at a later time.

A sample could be profiled before and after sputtering, and the results compared. The change in the profile, or curvature, could be caused by stress.

A wafer could be coated with photoresist, and patterned with radial grooves. Then the depth of the grooves (and hence the photoresist thickness) could be profiled radially. Variations in the thickness could

help to determine the parameters in achieving a more homogeneous photoresist coating during the spinning process.

8.5 Improving the Patterning Process

In order to improve the adhesion of the photoresist to the thin film, an adhesion promoter is recommended (i.e. Silicon Resources Inc. AP300).

To improve the adhesion of the photoresist to the thin film, a hard-bake is performed. In order to remove the photoresist after a hard bake, a better stripper than acetone needs to be found. Most aggressive strippers are incompatible with metals.

The photoresist used in this study may not be the best choice for wet-etching purposes. The AZ 1500 series has a low Novalak resin fraction that results in significantly improved adhesion and very high photospeeds.

8.6 Arrangements for Automated Scanning

A scanning Kerr microscope could be arranged by using an x-y position controller as the sample holder. A small sample could be positioned between the pole faces of the magnet in the Kerr setup, and

moved by computer to scan its surface. This could reveal the domain patterns present on the thin film.

A rotating sample holder could also be used to measure the response of the material to the orientation of the applied magnetic field. A spot can be chosen on a sample with a grating etched in the NiFe thin film. When the sample is rotated, the effects of the applied magnetic field can be measured parallel and perpendicular to the grating pattern, and at angles in between.

8.7 Creating Many Small Rectangular Patterns

Figure 8-4 shows gaps that are generated in the etched lines due to the stepper motors. There is a brief pause before the motor “steps” to the next position, resulting in a variation of the exposure.

This technique could be utilized to create long arrays of rectangular structures. If the line size was smaller, and the velocity increased, the steps could be enlarged and the structures isolated. These structures could be explored for the purpose of storing digital data.

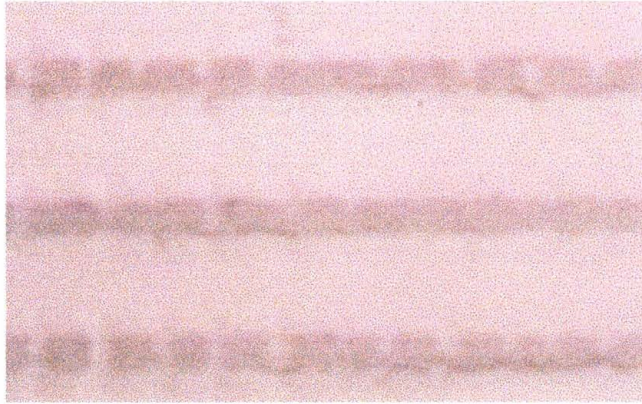
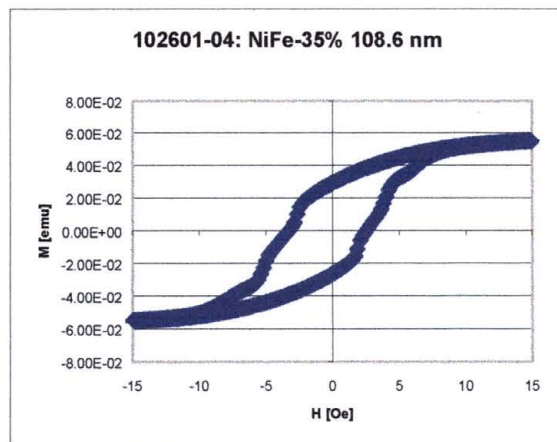
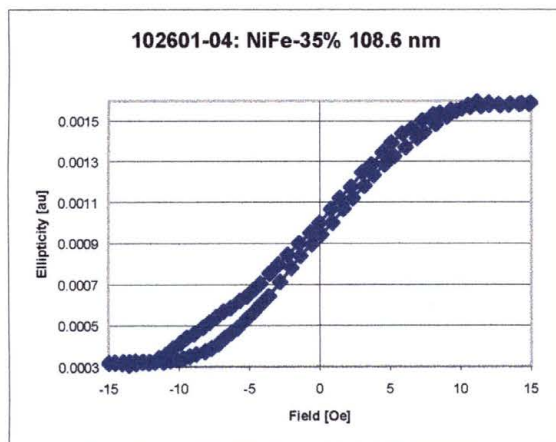
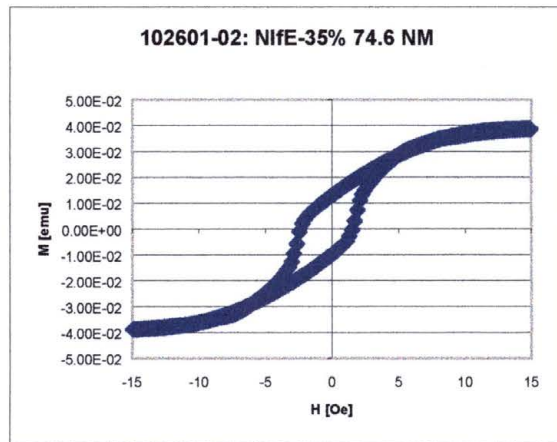
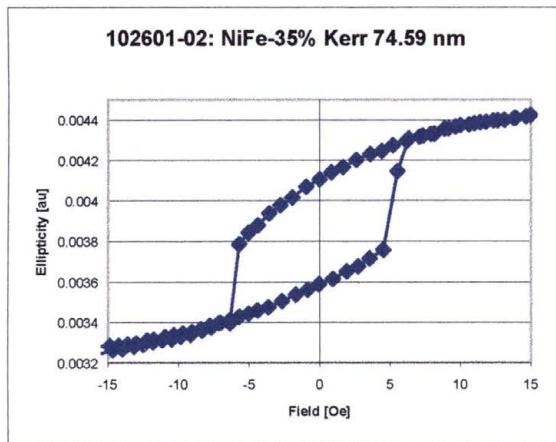
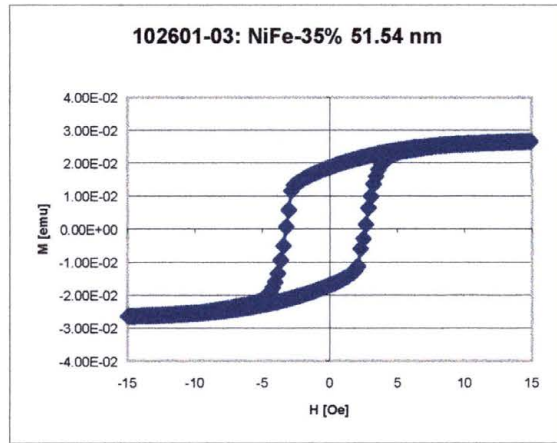
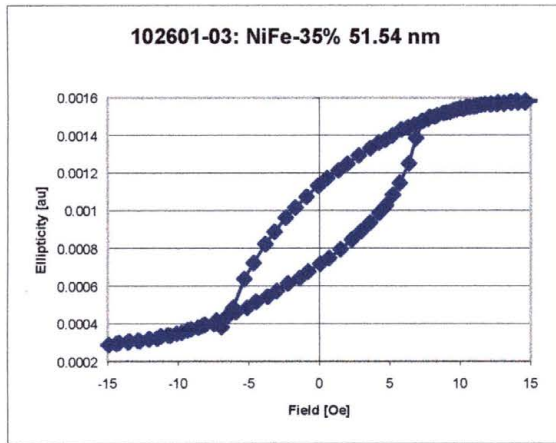
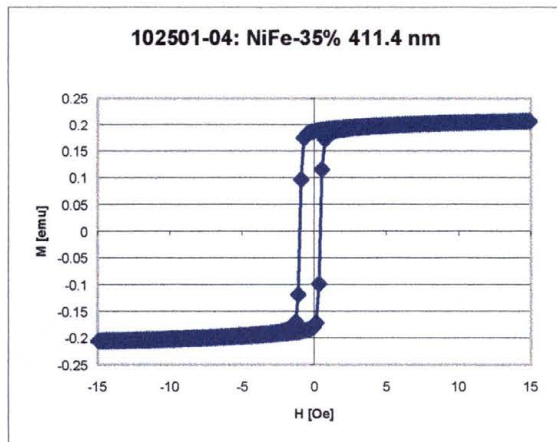
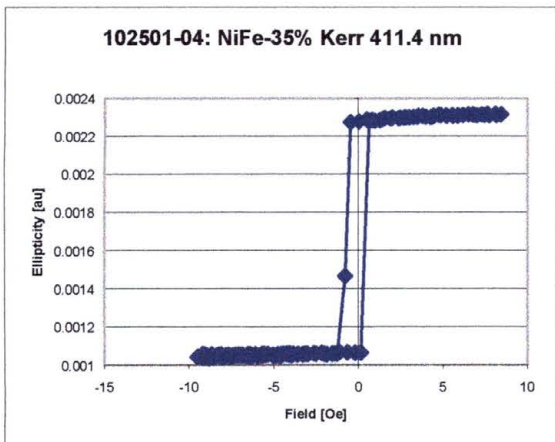
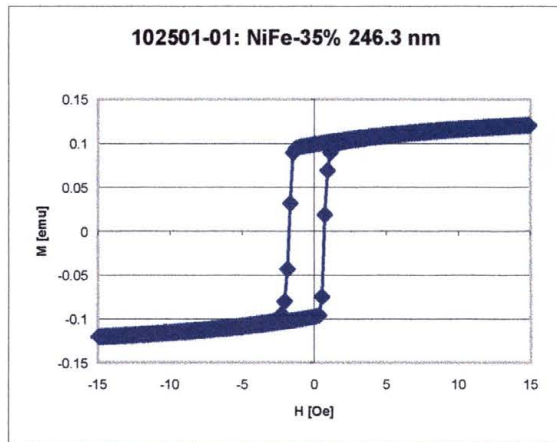
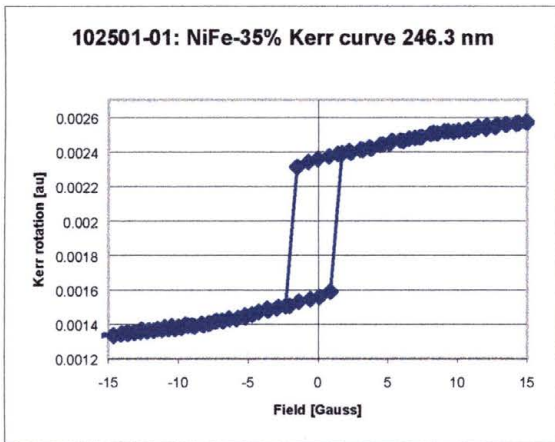
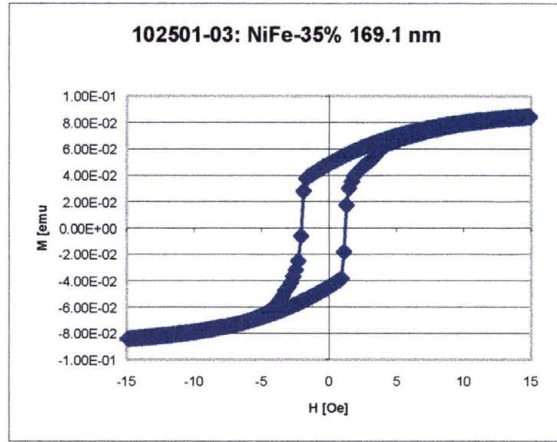
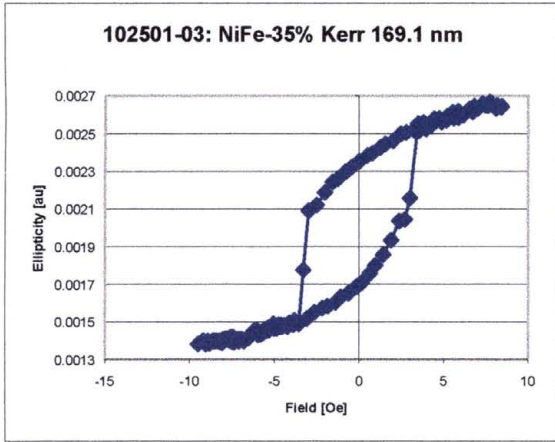
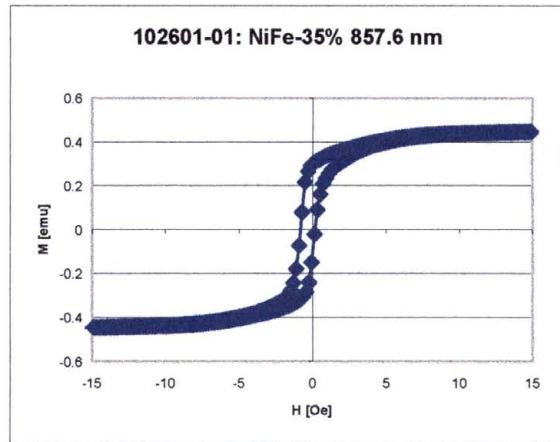
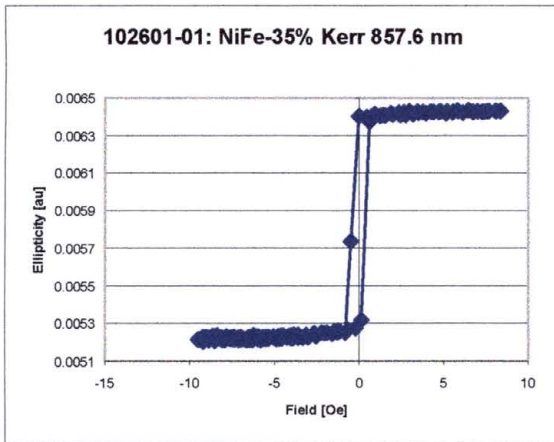
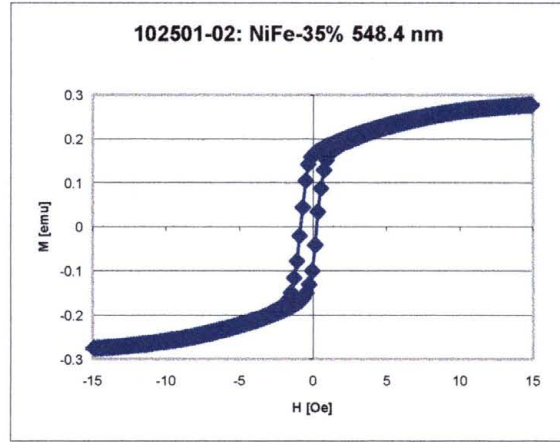
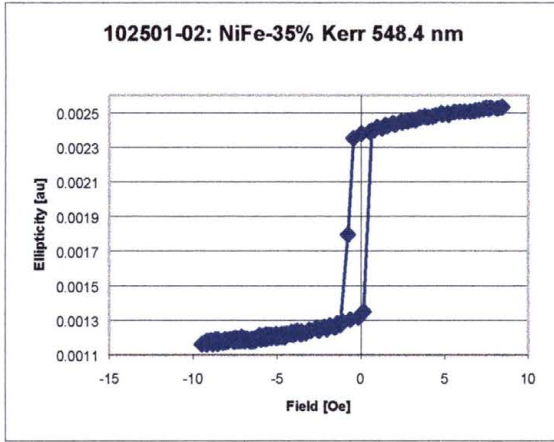


Figure 8-4 Gaps in the etched lines were created by the stepper motor

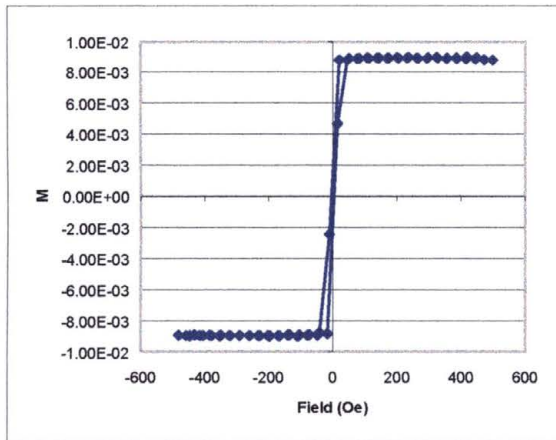
APPENDIX A Kerr and VSM Hysteresis Loops



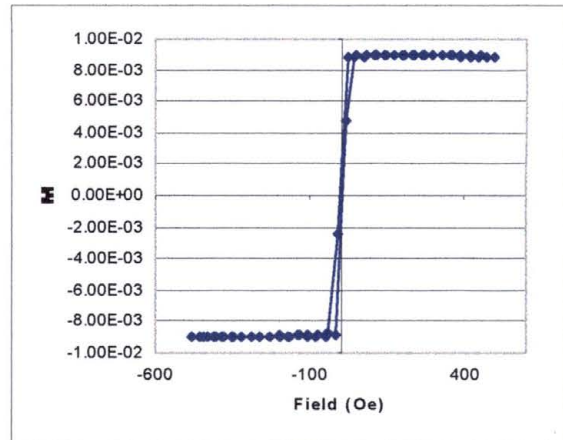




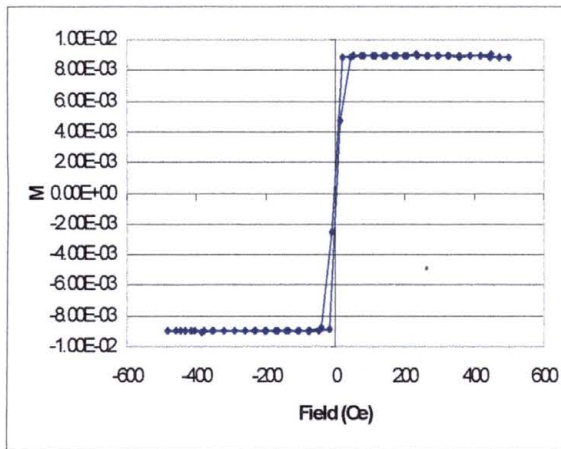
Appendix B Etch Series



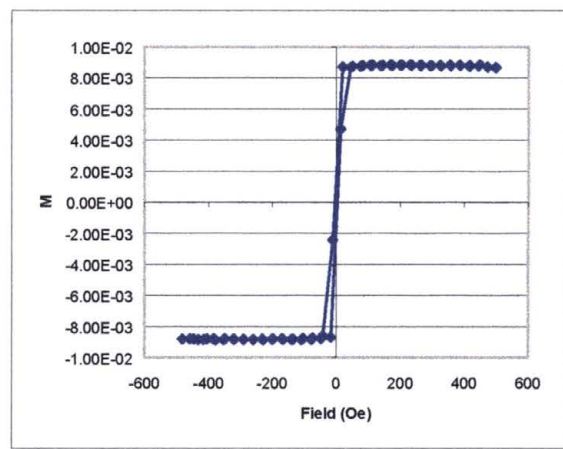
0s



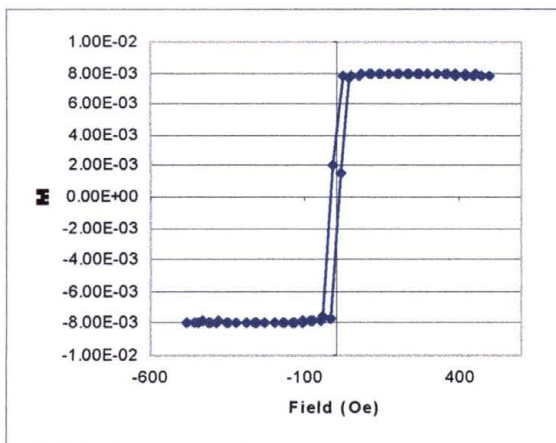
15s



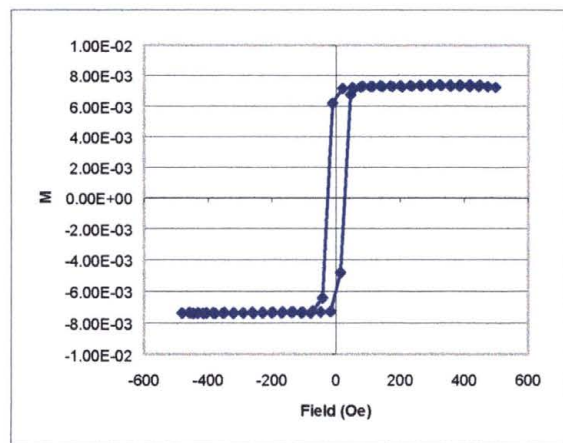
30s



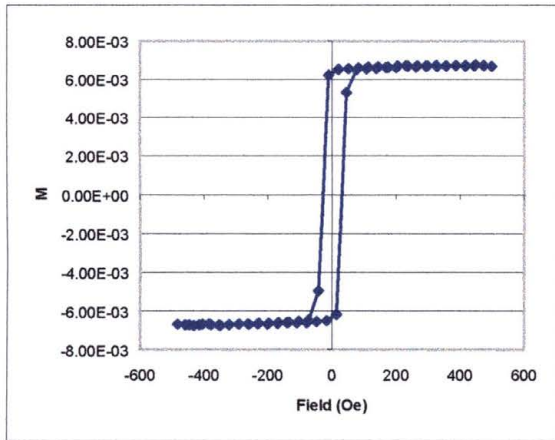
45s



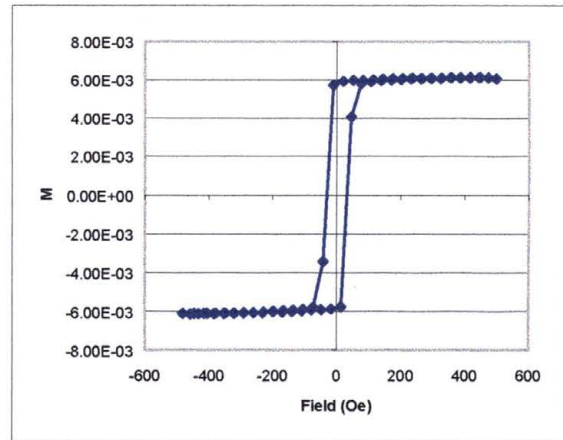
1m 15s



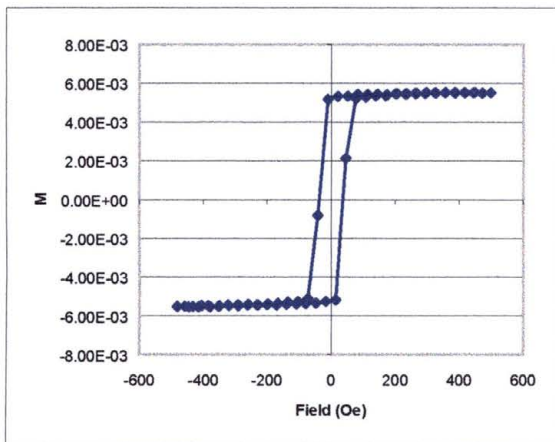
1m 30s



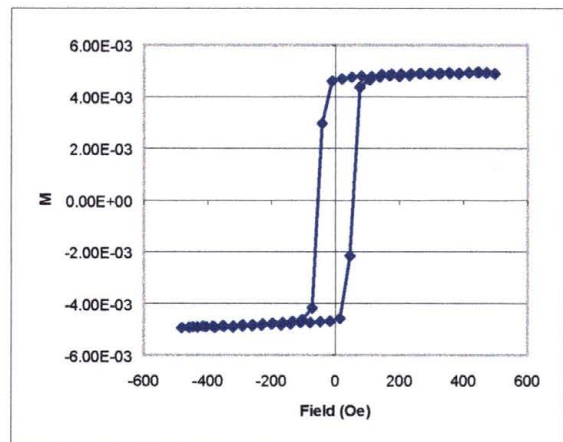
1m 45s



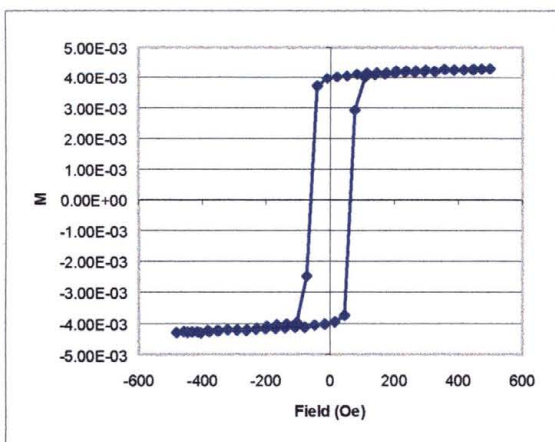
2m



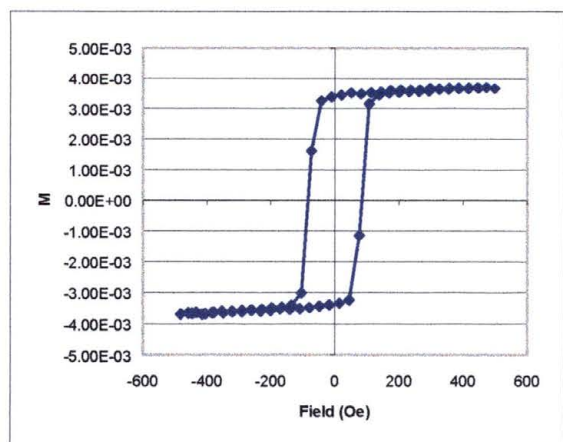
2m 15s



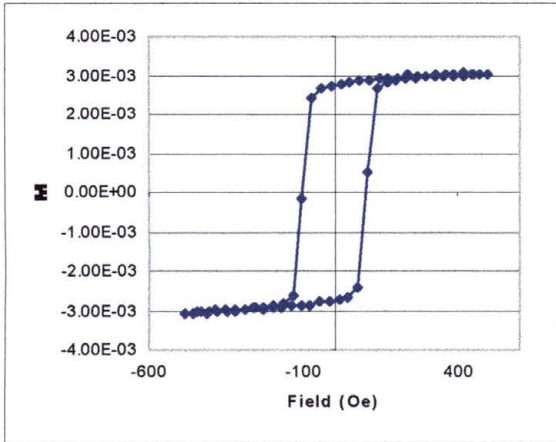
2m 30s



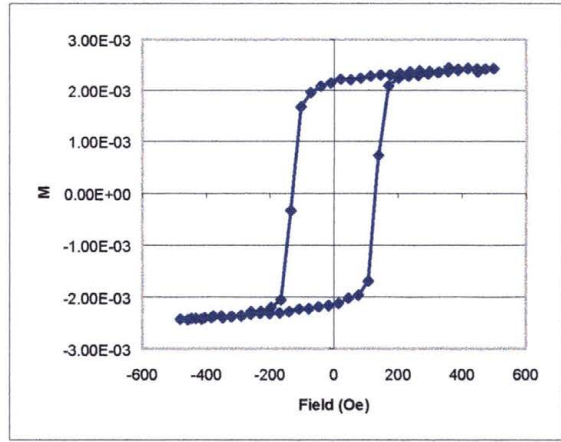
2m 45s



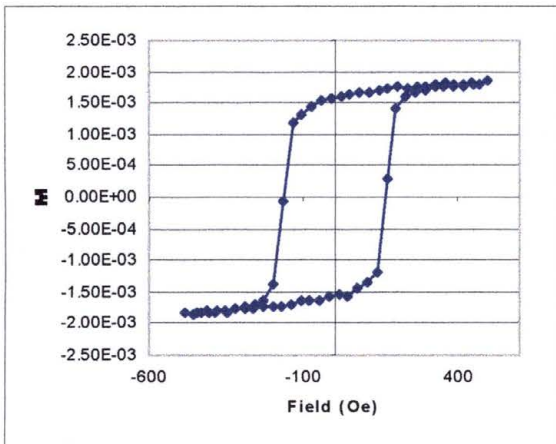
3m



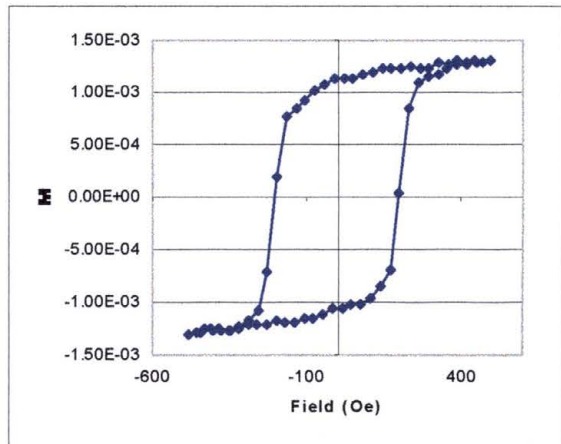
3m 15s



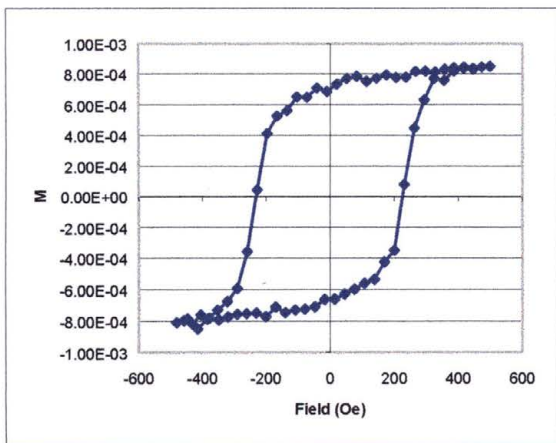
3m 30s



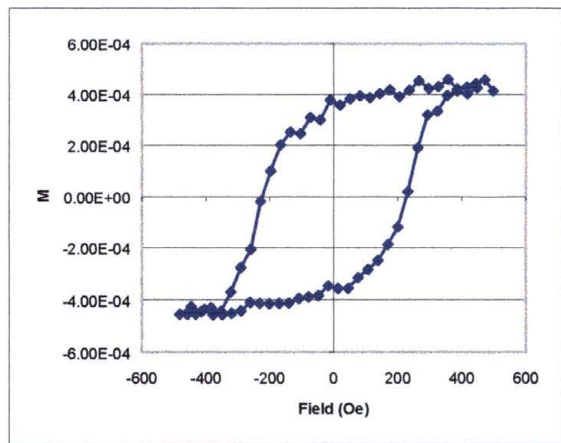
3m 45s



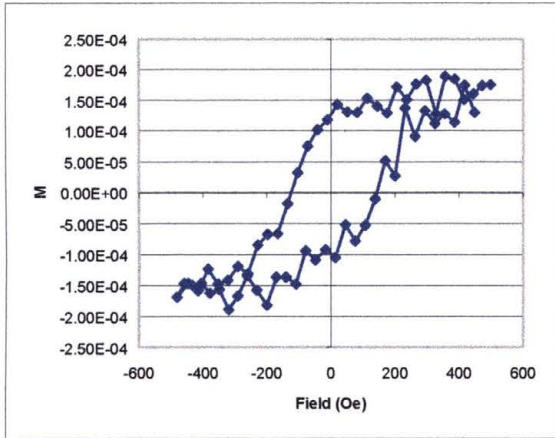
4m



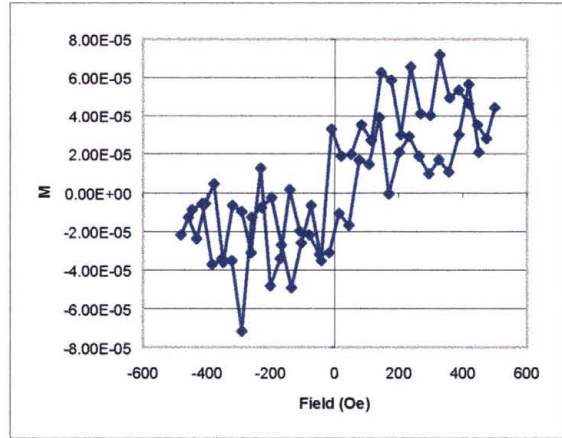
4m 15s



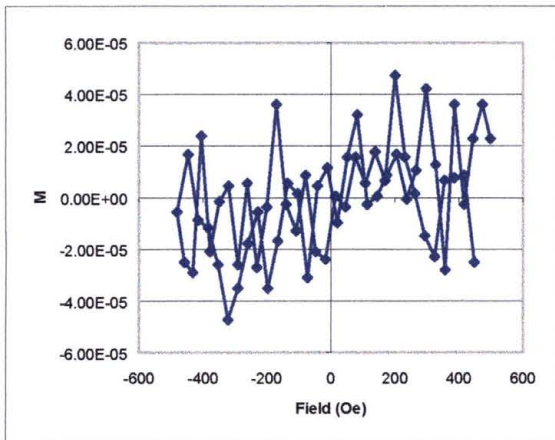
4m 30s



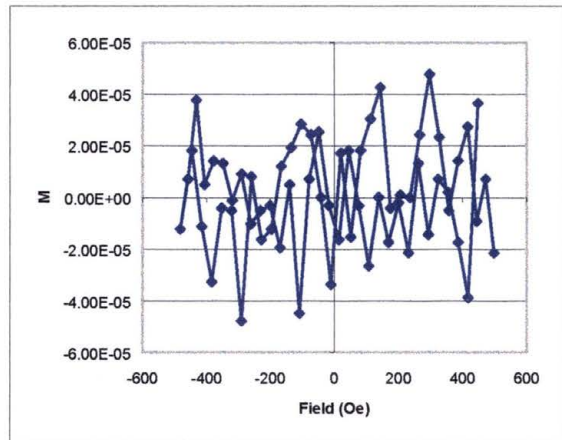
4m 45s



5m



5m 15s



5m 30s

Appendix C Photolithography Procedure

The photolithography process must take place in yellow light, since the photoresist is most sensitive to blue light. For this reason, it is necessary to use the yellow room lights when handling the photoresist or samples before they are developed and rinsed.

Spin

1) Turn on the EchoTherm HP-30 hotplate by the switch on the rear panel. It will beep and the display will light up. The display will show an "A" to indicate Actual temperature, and a "T" to indicate Target temperature. After pressing the hotplate temperature icon, the up and down arrows can be used to set the plate temperature. Set the temperature to 90° C. The display will toggle between the target and actual temperature.

2) Bake your sample to dehydrate it for 60s at 90° C.

3) The spinner is used for spinning other chemicals (D-Limonene), so it is necessary to make sure the spinner is clean before using it for spinning photoresist. Acetone may be used to clean the white plastic of the spinner. Do not use acetone on the clear plastic on the lid.

4) Attach the small chuck to the spinner. This chuck is used to hold samples that are 2-3 cm on each side. The rubber O-ring in the center of the chuck should be smaller than the sample. The O-ring is used to hold the sample by vacuum. There is a larger chuck for holding wafers while spinning.

5) Make sure the 3" exhaust hose is attached to the spinner and exhausts under the ventilation hood. Plug in the gray Gast vacuum pump to provide a vacuum for holding the sample to the chuck.

6) After the sample has cooled from the dehydration bake, set it on the chuck and turn the vacuum on by pressing the Vacuum button on the spinner control panel. The vacuum that holds the sample is monitored by a safety interlock. If the vacuum is insufficient, the word "Vacuum" will blink on the display, and you will be unable to spin. Close the lid on the spinner. The lid is also monitored by a safety interlock, and the spinner will not operate while it is open.

4) Select program B by using the arrow keys on the spinner. This program will spin at 3,000 rpm for 30s.

5) Dispense 1 ml of AZ 5214-E photoresist onto the sample, and immediately start the spinner with the RUN/STOP button.

6) After the spinner stops, remove the sample and place it on the hotplate for 60s at 90°C. This will harden the photoresist for processing.

Do not bake the sample again or expose it to white light until it has been developed and rinsed for the last time.

Develop

The sample to be developed is fastened into plastic locking tweezers. The plastic will not interact with the developer, and when the sample is locked in, it will not fall out during processing.

The sample is processed for 1 minute with an agitation of 1 revolution per second.

After processing, the sample is rinsed in a beaker full of DI water with slight agitation (1 per second) for 1 minute. After rinsing, the sample is dried by blowing it off with nitrogen. It is suggested that the sample stay in the DI water until it is moved to the area where it can be dried in nitrogen. Then the water does not have a chance to dry at all, but is blown off.

If the structure shows signs of underdevelopment or underexposure, developing time may be extended. This is done by placing the sample back in developer for 30s, and repeating the rinse and drying process. Note that additional development will have a smaller effect than the initial development. The developer will also degrade the quality of the photoresist with repeated development. Microscopic examination will show that the photoresist looks pitted or dirty after repeating the development process more than three times.

Etching

1) Bake the sample for 5 minutes at 90° C. If the sample is baked too hot (115° C) the photoresist cannot be removed by soaking in acetone. If the sample is not baked, the photoresist will be dissolved by the etchant.

2) Place the sample into plastic locking tweezers. Use a narrow beaker so that the sample can be suspended into the etchant. Figure C-1 shows an example arrangement.



Figure C-1 A sample suspended in etchant.

3) Estimate the etch time. For the diluted Al etch, the etch rate was determined to be 5.6 Å/s. Determine the thickness of the film from

the sputtering time. Then the etch time can be estimated by dividing by the etch rate. This will give an approximation of the actual etch time.

4) Place the sample in the etchant for the estimated time.

5) Rinse the sample in a beaker full of DI water for 60s with agitation of 1 rpm.

After etching, the sample is rinsed, dried and examined under a microscope. If the etch was incomplete, etching may be continued as long as the photoresist does not show signs of weakness or mobility. For gratings, this can be observed by the lines sagging in the center of the structure.

Endpoint detection can be used in etching. For the combination of NiFe 35% or NiFe 45% and diluted Al etchant, the following procedure can be used:

1) After exposing the sample in the laser writer, put the sample in an optical microscope. Find an area next to the edge of the sample that is away from the patterns exposed in the laser writer. The yellow filter of the microscope can be used to avoid further expose of the sample.

2) Focus at a power of 50x, and increase the light intensity to maximum.

3) Switch the yellow filter to clear for 1 minute, and then back to yellow.

4) Develop the sample.

This procedure creates a small circular spot where the photoresist is completely removed from the sample. When etching the sample, if this spot is closely monitored using an estimated etch time, it will turn dark brown for a few seconds before the metal film is completely etched away.

Appendix D Laser Writer Software Procedure

Turn on the System Power (on the laser power supply)

Turn on the Computer

Turn on the monitor

In the folder "New Stepmotor Code" double-click stepmotor.exe

After starting the program, you should see the command prompt:

PC3XCOMM V1.0 interactive mode (Press F1 for help):

At this point, the arrow keys may be used to position the sample. The arrow keys on the keypad move in large increments (80 microns), and the arrow keys between the numeric keypad and the alphabetic keypad move in small increments (2 microns).

The F9 and F10 keys have also been programmed to toggle between the 5x and 100x objective lenses. F9 is the “zoom in” key and F10 is the “zoom out” key. By centering the alignment beam on a structure at 5x, when the F9 key is pressed and the lens rotated to 100x, the structure should be in the 100x field of view.

To execute a command file, press F5, type in the name of the command file, and press ENTER.

Hit the F5 key (to run a command file)

Enter the filename LASEROFF.TXT and hit return

(This is to make sure the laser is off before beginning)

Turn on the Laser Power (on the power supply)

Turn the key to start the laser on the laser control box 180 degrees, until the ENABLED L.E.D. lights

It will take the laser a minute to start, you may hear a soft, high-pitched click

Place the sample into the laser writer

Table D-1 is a suggested procedure to etch three grating patterns. It lists the aperture, file name and laser power for each command file to be executed.

<i>Aperture</i>	<i>File Name</i>	<i>Laser Power</i>
	RESETZERO.TXT	
	AUTOCALIBRATE.TXT	
	FOCUSTEST.TXT	
200x20	EXPOSURETEST-V1000.TXT	140mW
80x40	EXPOSURETEST-V2000.TXT	140mW
80x40	GRATING-P10-V20000.TXT	140mW
200x20	GRATING-P4-V20000.TXT	140mW

Table D-1 File listing for a procedure to etch grating patterns

RESETZERO.TXT:

Before calibration, this resets the position of the xy controller to (0,0). This is necessary to ensure accurate calibration of the focus.

AUTOCALIBRATE.TXT:

Before running this command file, the background beam should be fully extinguished, and the alignment beam should be adjusted to full brightness. These potentiometers are located on the right side of the microscope. This is because the command file uses the autofocus command, which works best when there is an isolated bright area to focus on.

The command file will move to four points on a square, and auto-focus at each point. It will then return to the starting position.

After the focus data for the four points has been collected, the focus information will be saved to a file, and the command file will terminate.

FOCUSTEST.TXT:

This command file tests the focus at each of the four points on the square that was just measured. It will use the calculated slope of the sample determined from the points measured. If the focus at one or all of the points is fuzzy, then the sample may need to be adjusted or secured. The focus knob should be checked where the stepper motor is attached, to make sure that it is secure, and not slipping.

EXPOSURETEST-V1000.TXT:

This command file will draw a series of 6 lines, each at a different velocity, starting at 1000 steps/sec. The lines in the series are exposed at velocities of 1000, 2000, 5000, 10000, 20000 and 50000. Therefore, the lines will be exposed at decreasing levels of energy. The size of the spot is adjusted by the aperture setting.

After developing, if the velocities that the gratings were exposed at were too high or too low (the gratings were under or over exposed), then these patterns may be observed to select the correct velocity.

EXPOSURETEST-V2000.TXT.TXT:

This command file will generate the exposure test lines starting at a velocity of 2,000 steps/sec. It performs similar to the EXPOSURETEST-V1000.TXT command file. The only difference is that the velocities are 2000, 5000, 10000, 20000, 50000 and 100000.

GRATING-P10-V20000.TXT

GRATING-P4-V20000.TXT:

These files generate gratings. The 10-10ax2.txt file generates a grating with a beam size of 10 microns, and a pitch of 10 microns. The 5-4ax2.txt file generates a grating with a beam size of 5 microns, and a pitch of 4 microns. The first number in the file name is the beam size in microns. The second is the pitch in microns. So the file 5-2ax10.txt would generate a grating using a beam size of 5, and a pitch of 2 microns. The x2 on the end of the file name means "times 2" or twice as fast. This is because a rectangle is being used as the shape of the beam to expose the line patterns.

You may notice that the aperture for the file 10-10ax2.txt is 80x40. This corresponds to a rectangle that is twice as wide as it is high. Therefore, the velocity is twice as fast to expose the line, as compared to a square of 40x40. The exposures are based on square beam sizes because lines can be drawn in the vertical and horizontal directions with a square.

Appendix E Laser Wavelength Selection

The Argon laser has an output consisting of several bands of energy. However, the photoresist is most sensitive to the deep blue to ultraviolet spectrum.

It is critically important to observe laser safety when adjusting the variable interference filter to select a laser line. This can be difficult while wearing laser safety goggles. The following procedure is suggested:

- 1) Use a test sample coated with photoresist.
- 2) Adjust the laser to low power (50 mW).
- 3) Adjust the interference filter to the far end of its blue spectrum.
- 4) Initiate a scanning pattern with the computer. This can be a procedure that creates a grating.
- 5) While the laser writer is scanning and writing, adjust the interference filter until photoluminescence is observed. The following image shows photoluminescence. The image on the right shows the intensity of the beam observed during photoluminescence. Since the laser wavelength has been selected by the interference filter to be in the blue range, and red filters are used in the microscope, the laser light cannot be seen at all in the images. The image on the left of Figure E-1 is due to an alignment beam. The image on the right is the alignment beam plus the observed photoluminescence.

The photoluminescence is visible since it is at a different wavelength than the absorbed radiation.

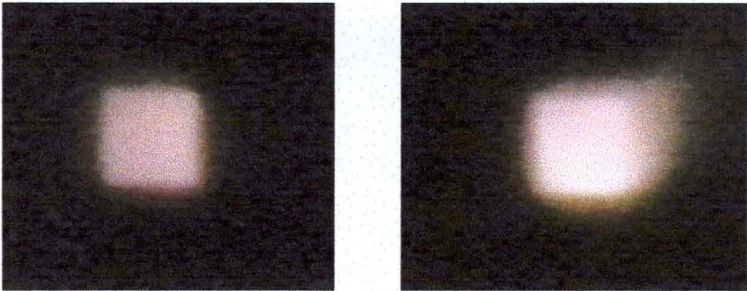


Figure E-1 Example of photoluminescence

VITA

Claude H. Garrett IV was born in Austin, Texas, on January 26, 1963, the son of Jean Evelyn Garrett and Claude H. Garrett III. After graduating from Round Rock High School in 1981, he worked for Motorola. He completed a Bachelor of Science degree from Southwest Texas State University in 1990, and continued to work for Dell and then the Texas Department of Human Services. In the Fall of 2000, he returned to the Graduate School of Southwest Texas State University.

Permanent Address: 13404 Rossello
Austin, TX 78729

This thesis was typed by Claude H. Garrett IV.

BIBLIOGRAPHY

¹ Garshelis, I. J. "Force transducers based on the stress dependence of coercive force"

² Haast, M.A.M. "Patterned magnetic thin films for ultra high density recording" Ph.D. Thesis, University of Twente, The Netherlands, 1999.

³ "Optics and Optical Instruments catalog" Edmund Industrial Optics, 2002.

⁴ Watts, Charles "A Biaxial Magneto-Optical Kerr Magnetometer For Studying Magnnetic Thin Films" Thesis, Southwest Texas State University 2000.

⁵ Jiles, David *Introduction to Magnetism and Magnetic Materials* Second Edition, Chapman and Hall, 1998.

⁶ AZ 5214 E Product Data Sheet, Clariant Corp.

⁷ Harry J. Levinson, *SEMI lithography Science – SEMICON SouthWest 99*, 1999.

⁸ AZ400K Product Data Sheet, Clariant Corp., 1997.

⁹ <http://www.enme.umd.edu/mml/SOP/photoresist.html>, accessed 4/17/2002.

¹⁰ 5200AZ Product Data Sheet, Clariant Corp.

¹¹ AZ 5200-E-IR Application Note, Clariant Corp.

-
- ¹² Groenland, J.P.J. “Thin-Film Magnetoresistive Absolute Position Detector” Ph.D. Thesis, University of Twente, Enschede (The Netherlands) 1990.
- ¹³ Harland G. Thompkins, *A User Guide to Ellipsometry*.
- ¹⁴ B. D. Cullity, *Introduction to Magnetic Materials*. Addison Wesley Publishing Company, 1972.
- ¹⁵ www.crystran.co.uk/sidata.htm, April 18, 2002
- ¹⁶ Rolf E. Hummel, *Electronic Properties of Materials*. Second Edition. Springer-Verlag, 1993.

